CHAPTER 28

ACID-BASE PHYSIOLOGY

Walter F. Boron

Acid-base physiology is really the study of the proton, or hydrogen ion (H^+). Although they are present in exceedingly low concentrations in most intracellular and extracellular fluids, protons nevertheless have a major impact on biochemical reactions and on a variety of physiological processes that are critical for the homeostasis of the entire body and individual cells. Not surprisingly, the body has evolved sophisticated systems to maintain $[H^+]$ values within narrow and precise ranges in the blood plasma, intracellular fluid, and other compartments.

This chapter provides the introduction to acid-base physiology, including the chemistry of buffers, the CO_2/HCO_3^- buffer system, the competition between the CO_2/HCO_3^- buffer system and other buffers, and the regulation of intracellular pH. In other chapters, we discuss how blood pH—and, by extension, the pH of extracellular fluid—is under the dual control of the respiratory system, which regulates plasma $[CO_2]$ (see Chapter 31), and the kidneys, which regulate plasma $[HCO_3^-]$ (see Chapter 39). In addition, we discuss the control of cerebrospinal fluid pH in Chapter 32.

pH AND BUFFERS

pH values vary enormously among different intracellular and extracellular compartments

According to Brønsted's definition, an **acid** N28-1 is any chemical substance (e.g., CH_3COOH, NH_4^+) that can donate an H^+. A **base** is any chemical substance (e.g., CH_3COO^-, NH_3) that can accept an H^+. The term **alkali** can be used interchangeably with **base.**

$[H^+]$ varies over a large range in biological solutions, from >100 mM in gastric secretions to <10 nM in pancreatic secretions. In 1909, the chemist Sørensen introduced the **pH scale** in an effort to simplify the notation in experiments in which he was examining the influence of $[H^+]$ on enzymatic reactions. He based the pH scale on powers of 10: N28-2

$$pH \equiv -\log_{10}[H^+] \qquad \textbf{(28-1)}$$

Thus, when $[H^+]$ is 10^{-7} M, the pH is 7.0. The higher the $[H^+]$, the lower the pH (Table 28-1). It is worth remembering that a 10-fold change in $[H^+]$ corresponds to a pH shift of 1, whereas a 2-fold change in $[H^+]$ corresponds to a pH shift of ~0.3.

Even small changes in pH can have substantial physiological consequences because most biologically important molecules contain chemical groups that can either donate an H^+ (e.g., $R–COOH \rightarrow R–COO^- + H^+$) and thereby act as a weak acid, or accept an H^+ (e.g., $R–NH_2 + H^+ \rightarrow R–NH_3^+$) and thus behave as a weak base. To the extent that these groups donate or accept protons, a pH shift causes a change in net electrical charge (or valence) that can, in turn, alter biological activity either directly (e.g., by altering the affinity for a charged ligand) or indirectly (e.g., by altering molecular conformation).

pH-sensitive molecules include a variety of enzymes, receptors and their ligands, ion channels, transporters, and structural proteins. For most proteins, pH sensitivity is modest. The activity of the Na-K pump (see pp. 115–117), for example, falls by about half when the pH shifts by ~1 pH unit from the optimum pH, which is near the resting pH of the typical cell. However, the activity of phosphofructokinase, a key glycolytic enzyme (see p. 1176), falls by ~90% when pH falls by only 0.1. The overall impact of pH changes on cellular processes can be impressive. For example, cell proliferation in response to mitogenic activation is maximal at the normal, resting intracellular pH but may fall as much as 85% when intracellular pH falls by only 0.4.

Table 28-2 lists the pH values in several body fluids. Because the pH of neutral water at 37°C is 6.81, most major body compartments are alkaline.

Buffers minimize the size of the pH changes produced by adding acid or alkali to a solution

A **buffer** is any substance that reversibly consumes or releases H^+. In this way, buffers help to stabilize pH. Buffers do not *prevent* pH changes, they only help to *minimize* them.

Consider a hypothetical buffer B for which the protonated form $HB^{(n+1)}$, with a valence of $n + 1$, is in equilibrium with its deprotonated form $B^{(n)}$, which has the valence of n:

$$HB^{(n+1)} \rightleftarrows B^{(n)} + H^+ \qquad \textbf{(28-2)}$$

Here, $HB^{(n+1)}$ is a **weak acid** because it does not fully dissociate; $B^{(n)}$ is its **conjugate weak base.** Conversely, $B^{(n)}$ is a **weak base** and $HB^{(n+1)}$ is its conjugate weak acid. The **total buffer**

N28-1 Hydrogen Ions in Aqueous Solutions

Contributed by Emile Boulpaep and Walter Boron

Hydrogen ions do not truly exist as "free" protons in aqueous solutions. Instead, a shell of water molecules surrounds a proton, forming an extended complex sometimes denoted as H_3O^+ (hydronium ion) or $H_9O_4^+$. Nevertheless, for practical purposes, we will treat the proton as if it were free. Also—as we do elsewhere in this book—we shall refer to *concentrations* of H^+, bicarbonate (HCO_3^-), and other ions. Bear in mind, however, that it is more precise to work with ion **activities** (i.e., the effective concentrations of ions in realistic, nonideal solutions).

N28-2 Origin of the *p* of pH

Contributed by Walter Boron

Although the conventional wisdom is that the *p* of pH stands for the *power of 10,* Norby's analysis of Sørensen's original papers reveals a far more accidental explanation.

Sørensen used *p* and *q* to represent two solutions in an electrometric experiment. He arbitrarily assigned the standard *q* solution an $[H^+]$ of 1 *N* (normal). That is, his standard solution had an $[H^+]$ of 1 *N*, which is $C_q = 10^{-q}$. His unknown, therefore, had an $[H^+]$ of $C_p = 10^{-p}$. Using this approach, Sørensen proposed the nomenclature p^+_H … and nowadays, we use simply pH.

REFERENCES

Norby JG: The origin and the meaning of the little p in pH. Trends Biochem Sci 25:36–37, 2000.

Sørensen SPL: Enzymstudien. II. Mitteilung. Über die Messung und die Bedeutung der Wasserstoffionenkoncentration bei enzymatischen Prozessen. Biochem Z 21:131–304, 22:352–356, 1909.

Sørensen SPL: Études enzymatiques. II. Sur la mesure et l'importance de la concentration des ions hydrogène dans les réactions enzymatiques. C R Lab Carlsberg 8:1–168, 1909.

We thank Christian Aalkjaer of the University of Aarhus in Denmark for bringing Norby's paper to our attention.

TABLE 28-1 Relationship between [H⁺] and pH Values

	[H⁺] (m)	pH	
×10	1×10^{-6}	6.0	1 pH unit
	1×10^{-7}	7.0	
	1×10^{-8}	8.0	
×2	8×10^{-8}	7.1	0.3 pH unit
	4×10^{-8}	7.4	
	2×10^{-8}	7.7	
	1×10^{-8}	8.0	

TABLE 28-2 Approximate pH Values of Various Body Fluids

COMPARTMENT	pH
Gastric secretions (under conditions of maximal acidity)	0.7
Lysosome	5.5
Chromaffin granule	5.5
Neutral H_2O at 37°C	6.81
Cytosol of a typical cell	7.2
Cerebral spinal fluid (CSF)	7.3
Arterial blood plasma	7.4
Mitochondrial inner matrix	7.5
Secreted pancreatic fluid	8.1

concentration, [TB], is the sum of the concentrations of the protonated and unprotonated forms:

$$[TB]=[HB^{(n+1)}]+[B^{(n)}] \quad \textbf{(28-3)}$$

The valence of the acidic (i.e., protonated) form can be positive, zero, or negative:

$$\begin{aligned} &\overbrace{NH_4^+}^{\text{Weak acid } (HB^{(n+1)})} \rightleftarrows \overbrace{NH_3}^{\text{Conjugate weak base } (B^{(n)})} + H^+ \\ &H_2CO_3 \rightleftarrows HCO_3^- + H^+ \\ &H_2PO_4^- \rightleftarrows HPO_4^{2-} + H^+ \end{aligned} \quad \textbf{(28-4)}$$

In these examples, NH_4^+ (ammonium), H_2CO_3 (carbonic acid), and $H_2PO_4^-$ ("monobasic" inorganic phosphate) are all weak acids, whereas NH_3 (ammonia), HCO_3^- (bicarbonate), and $H_2PO_4^{2-}$ ("dibasic" inorganic phosphate) are the respective conjugate weak bases. Each buffer reaction is governed by a **dissociation constant,** K

$$K=\frac{[B^{(n)}][H^+]}{[HB^{(n+1)}]} \quad \textbf{(28-5)}$$

If we add to a physiological solution a small amount of HCl—which is a strong acid because it fully dissociates—the buffers in the solution consume almost all added H^+:

$$H^+ + Cl^- + B^{(n)} \rightarrow HB^{(n+1)} + Cl^- \quad \textbf{(28-6)}$$

For each H^+ buffered, one $B^{(n)}$ is *consumed.* The tiny amount of H^+ that is *not buffered* remains free in solution and is responsible for a decrease in pH.

If we instead titrate this same solution with a strong base such as NaOH, H^+ derived from $HB^{(n+1)}$ neutralizes almost all the added OH^-:

$$Na^+ + OH^- + HB^{(n+1)} \rightarrow Na^+ + B^{(n)} + H_2O \quad \textbf{(28-7)}$$

For each OH^- buffered, one $B^{(n)}$ is *formed.* The tiny amount of added OH^- that is not neutralized by the buffer equilibrates with H^+ and H_2O and is responsible for an increase in pH. N28-3

A useful measure of the strength of a buffer is its **buffering power (β),** which is the number of moles of strong base (e.g., NaOH) that one must add to a liter of solution to increase pH by 1 pH unit. This value is equivalent to the amount of strong acid (e.g., HCl) that one must add to decrease the pH by 1 pH unit. Thus, buffering power is

$$\beta \equiv \frac{\overbrace{\Delta[\text{Strong base}]}^{\text{moles/liter}}}{\Delta pH} = -\frac{\overbrace{\Delta[\text{Strong acid}]}^{\text{moles/liter}}}{\Delta pH} \quad \textbf{(28-8)}$$

In the absence of CO_2/HCO_3^-, the buffering power of whole blood (which contains erythrocytes, leukocytes, and platelets) is ~25 mM/pH unit. This value is known as the **non-HCO_3^- buffering power ($\beta_{\text{non-}HCO_3^-}$).** In other words, we would have to add 25 mmol of NaOH to a liter of whole blood to increase the pH by 1 unit, assuming that β is constant over this wide pH range. For blood plasma, which lacks the cellular elements of whole blood, $\beta_{\text{non-}HCO_3^-}$ is only ~5 mM/pH unit, which means that only about one fifth as much strong base would be needed to produce the same pH increase.

According to the Henderson-Hasselbalch equation, pH depends on the ratio $[CO_2]/[HCO_3^-]$

The most important physiological buffer pair is CO_2 and HCO_3^-. The impressive strength of this buffer pair is due to the volatility of CO_2, which allows the lungs to maintain stable CO_2 concentrations in the blood plasma despite ongoing metabolic and buffer reactions that produce or consume CO_2. Imagine that a beaker contains an aqueous solution of 145 mM NaCl (pH = 6.81), but no buffers. We now expose this solution to an atmosphere containing CO_2 (Fig. 28-1). The concentration of dissolved CO_2 ($[CO_2]_{dis}$) is governed by **Henry's law** (see Box 26-2):

$$[CO_2]_{dis} = s \cdot P_{CO_2} \quad \textbf{(28-9)}$$

At the temperature (37°C) and ionic strength of mammalian blood plasma, the **solubility coefficient,** ***s,*** is ~0.03 mM/mm Hg. Because the alveolar air with which arterial blood equilibrates has a P_{CO_2} of ~40 mm Hg, or torr, $[CO_2]_{dis}$ in arterial blood is

$$[CO_2]_a = (0.03 \text{ mM/mm Hg}) \cdot 40 \text{ mm Hg} = 1.2 \text{ mM} \quad \textbf{(28-10)}$$

N28-3 Buffering of H^+

Contributed by Walter Boron

For each H^+ buffered in Equation 28-6, one $B^{(n)}$ is *consumed*. For each OH^- buffered in Equation 28-7, one $B^{(n)}$ is *formed*. Because almost all of the added H^+ or OH^- is buffered, the change in the concentration of the unprotonated form of the buffer (i.e., $\Delta[B^{(n)}]$) is a good index of the amount of strong acid or base added per liter of solution.

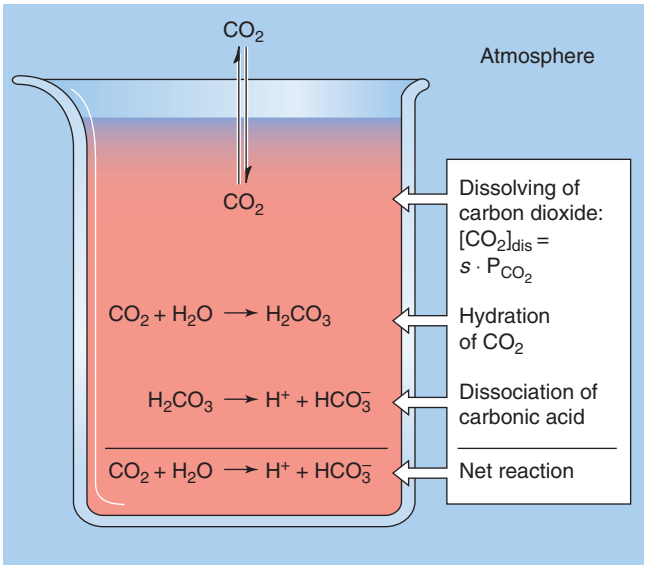

Figure 28-1 Interaction of CO_2 with water.

So far, the entry of CO_2 from the atmosphere into the aqueous solution has had *no effect* on pH. The reason is that we have neither generated nor consumed H^+. CO_2 itself is neither an acid nor a base. If we were considering dissolved N_2 or O_2, our analysis would end here because these gases do not further interact with simple aqueous solutions. The aqueous chemistry of CO_2, however, is more complicated, because CO_2 reacts with the solvent (i.e., H_2O) to form carbonic acid:

$$CO_2 + H_2O \xrightarrow{\text{slow}} H_2CO_3 \qquad \textbf{(28-11)}$$

This **CO_2 hydration reaction** is very slow. N28-4 In fact, it is far too slow to meet certain physiological needs. The enzyme **carbonic anhydrase,** N18-3 present in erythrocytes and elsewhere, catalyzes a reaction that effectively bypasses this slow hydration reaction. Carbonic acid is a weak acid that rapidly dissociates into H^+ and HCO_3^-:

$$H_2CO_3 \xrightarrow{\text{fast}} H^+ + HCO_3^- \qquad \textbf{(28-12)}$$

This **dissociation reaction** is the first point at which pH falls. Note that the formation of HCO_3^- (the conjugate weak base of H_2CO_3) necessarily accompanies the formation of H^+ in a stoichiometry of 1 : 1. The observation that pH decreases, even though the above reaction produces the weak base HCO_3^-, is sometimes confusing. A safe way to reason through such an apparent paradox is to focus always on the fate of the proton: if the reaction forms H^+, pH falls. Thus, even though the dissociation of H_2CO_3 leads to generation of a weak base, pH falls because H^+ forms along with the weak base.

Unlike the hydration of CO_2, the dissociation of H_2CO_3 is extremely fast. Thus, in the absence of carbonic anhydrase, the slow CO_2 hydration reaction limits the speed at which increased $[CO_2]_{dis}$ leads to the production of H^+. HCO_3^- can accept a proton to form its conjugate weak acid (i.e., H_2CO_3) or release a second proton to form its conjugate weak base (i.e., CO_3^{2-}). Because this latter reaction generally is of only minor physiological significance for buffering in mammals, we will not discuss it further.

We may treat the hydration and dissociation reactions that occur when we expose water to CO_2 as if only one reaction were involved:

$$\begin{aligned} &CO_2 + H_2O \rightleftarrows H_2CO_3 \rightleftarrows H^+ + HCO_3^- \\ &CO_2 + H_2O \rightleftarrows H^+ + HCO_3^- \end{aligned} \qquad \textbf{(28-13)}$$

Moreover, we can define a dissociation constant for this pseudoequilibrium:

$$K = \frac{[H^+][HCO_3^-]}{[CO_2]} \qquad \textbf{(28-14)}$$

In logarithmic form, this equation becomes N28-5

$$pH = pK + \log\frac{[HCO_3^-]}{[CO_2]} \qquad \textbf{(28-15)}$$

Finally, we may express $[CO_2]$ in terms of P_{CO_2}, recalling from Henry's law that $[CO_2] = s \cdot P_{CO_2}$:

$$pH = pK + \log\frac{[HCO_3^-]}{s \cdot P_{CO_2}} \qquad \textbf{(28-16)}$$

This is the **Henderson-Hasselbalch** equation, a logarithmic restatement of the CO_2/HCO_3^- equilibrium in Equation 28-14. Its central message is that pH depends not on $[HCO_3^-]$ or P_{CO_2} per se, but on their ratio. Human arterial blood has a P_{CO_2} of ~40 mm Hg and an $[HCO_3^-]$ of ~24 mM. If we assume that the pK governing the CO_2/HCO_3^- equilibrium is 6.1 at 37°C, then

$$pH = 6.1 + \log\frac{24\,\text{mM}}{(0.03\,\text{mM/mm Hg}) \times 40\,\text{mm Hg}} = 7.40 \qquad \textbf{(28-17)}$$

Thus, the Henderson-Hasselbalch equation correctly predicts the normal pH of arterial blood.

CO_2/HCO_3^- has a far higher buffering power in an open than in a closed system

The buffering power of a buffer pair such as CO_2/HCO_3^- depends on three factors:

1. **Total concentration of the buffer pair, [TB].** Other things being equal, β is proportional to [TB].
2. **The pH of the solution.** The precise dependence on pH will become clear below.
3. **Whether the system is open or closed.** That is, can one member of the buffer pair equilibrate between the "system" (the solution in which the buffer is dissolved) and the "environment" (everything else)?

If neither member of the buffer pair can enter or leave the system, then $HB^{(n+1)}$ can become $B^{(n)}$, and vice versa, but [TB] is fixed. This is a **closed system.** An example of a closed-system buffer is inorganic phosphate in a beaker of water, or a titratable group on a protein in blood plasma. In a closed system, the buffering power of a buffer pair is N28-6

N28-4 Out-of-Equilibrium CO_2/HCO_3^- Solutions

Contributed by Walter Boron

As described on page 629, adding CO_2 to an aqueous solution initiates a series of two reactions that, in the end, produce HCO_3^- and protons:

$$CO_2 + H_2O \xrightarrow{Slow} H_2CO_3 \xrightarrow{Fast} HCO_3^- + H^+ \quad \textbf{(NE 28-1)}$$

In the absence of carbonic anhydrase (CA), the first reaction—the hydration of CO_2 to form carbonic acid—is extremely slow. The second is extremely fast. At equilibrium, the overall rate of the two forward reactions must be the same as the overall rate of the reverse reactions:

$$CO_2 + H_2O \xleftarrow{Slow} H_2CO_3 \xleftarrow{Fast} HCO_3^- + H^+ \quad \textbf{(NE 28-2)}$$

The first of these reverse reactions is extremely rapid, whereas the second—the dehydration of H_2CO_3 to form CO_2 and water—is extremely slow in the absence of CA. As noted in the text, we can treat the system as if only one reaction were involved:

$$CO_2 + H_2O \rightleftharpoons HCO_3^- + H^+ \quad \textbf{(NE 28-3)}$$

Moreover, we can describe this pseudoreaction by a single equilibrium constant. As shown by Equation 28-15, we can describe the equilibrium condition in logarithmic form by the following equation:

$$pH = pK + \log_{10}\left(\frac{[HCO_3^-]}{[CO_2]}\right) \quad \textbf{(NE 28-4)}$$

In other words, considering only *equilibrium* conditions, it is impossible to change pH or $[HCO_3^-]$ or $[CO_2]$ one at a time. If we change one of the three parameters (e.g., pH), we must change at least one of the other two (i.e., $[HCO_3^-]$ or $[CO_2]$). Unfortunately, there are many cases in which the addition of CO_2 and HCO_3^- markedly enhances some process. For example, at identical values of intracellular pH, the activation of quiescent cells by mitogens is far more robust in the presence than in the absence of the physiological CO_2/HCO_3^- buffer. Which buffer component is critical in this case, CO_2 or HCO_3^-? There are also many cases in which a stress such as respiratory acidosis or metabolic acidosis triggers a particular response. For example, respiratory acidosis stimulates HCO_3^- reabsorption by the kidney—a metabolic compensation to a respiratory acidosis, as discussed beginning on pages 641–642 in the text. Again, we can ask which altered parameter signals the kidney to increase its reabsorption of HCO_3^-, the rise in $[CO_2]$ or the fall in pH?

In the 1990s, the laboratory of Walter Boron realized that it could exploit the slow equilibrium $CO_2 + H_2O \rightleftarrows H_2CO_3$ to create CO_2/HCO_3^- solutions that are temporarily *out of equilibrium*. eFigure 28-1*A* illustrates how one can make an out-of-equilibrium (OOE) "pure" CO_2 solution that contains a physiological level of CO_2, has a physiological pH, but contains virtually no HCO_3^-. The approach is to use a dual syringe pump to rapidly mix the contents of two syringes, each flowing at the same rate. One syringe contains a double dose of CO_2 (e.g., 10% CO_2) at a pH that is so low (e.g., pH 5.40) that, given a pK of ~6.1, very little HCO_3^- is present. The other syringe contains a well-buffered, relatively alkaline solution that contains no CO_2 or HCO_3^-. The pH of this second solution is chosen so that at the instant of mixing at the T connection, the solution has a pH of 7.40. Of course, the $[CO_2]$ after mixing is 5% (which corresponds to a P_{CO_2} of ~37 mm Hg), and the $[HCO_3^-]$ is virtually zero. The solutions flow so rapidly that they reach the cell of interest before any significant re-equilibration of the CO_2 and HCO_3^-. Moreover, a suction device continuously removes the solution. As a result, the cells are continuously exposed to a freshly generated OOE solution.

eFigure 28-1*B* illustrates how one could make the opposite solution—a "pure" HCO_3^- solution that has a physiological $[HCO_3^-]$ and pH but virtually no $[CO_2]$. The OOE approach can be used to make solutions with virtually any combination of $[CO_2]$, $[HCO_3^-]$, and pH—at least for moderate pH values. At extremely alkaline pH values, the reaction $CO_2 + OH^- \rightarrow HCO_3^-$ generates HCO_3^- so fast that it effectively short-circuits the OOE approach. Conversely, at extremely acid pH values, the rapid reaction $H^+ + HCO_3^- \rightleftarrows H_2CO_3$ creates relatively high levels of H_2CO_3 so that even the uncatalyzed reaction $H_2CO_3 \rightarrow CO_2 + H_2O$ is high enough to short-circuit the OOE approach. Nevertheless, at almost any pH of interest to physiologists, OOE technology allows one to change $[CO_2]$, $[HCO_3^-]$, and pH one at a time.

Work on renal proximal tubules with OOE solutions has shown that proximal tubules have the ability to sense rapid shifts in the CO_2 concentration of the basolateral (i.e., blood-side) solution that surrounds the outside of the tubule. This work suggests that the tubule has a sensor for CO_2 that is independent of any changes in pH or HCO_3^-. The tubule uses this CO_2-sensing mechanism in its response to respiratory acidosis (see pp. 637–638). This metabolic compensation involves a rapid increase in the rate at which it transports HCO_3^- from the tubule lumen to the blood, and thus a partial correction of the acidosis.

Work on neurons cultured from the hippocampus suggests that certain neurons can detect rapid decreases in the extracellular HCO_3^- concentration ($[HCO_3^-]_o$), independent of any changes in pH_o or $[CO_2]_o$. The cell may use this detection system to stabilize intracellular pH (pH_i) during extracellular metabolic acidosis, which would otherwise lower pH_i.

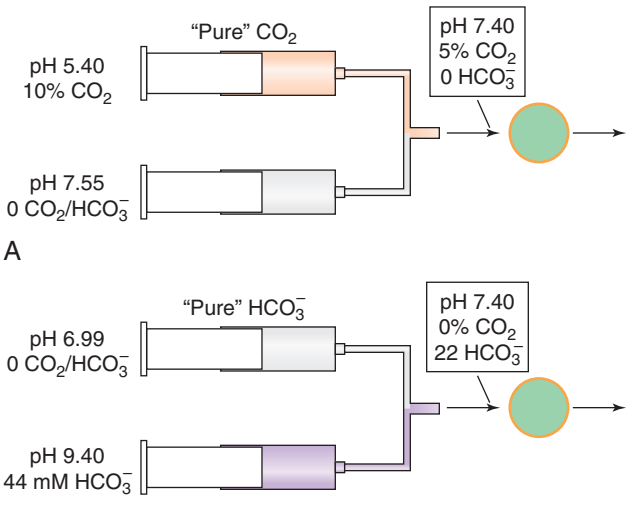

eFigure 28-1 Generation of out-of-equilibrium solutions. (Adapted from Zhao J, Hogan EM, Bevensee MO, et al: Out-of-equilibrium CO_2/HCO_3^- solutions and their use in characterizing a novel K/HCO_3 cotransporter. Nature 374:636–639, 1995.)

Continued

N28-4 Out-of-Equilibrium CO_2/HCO_3^- Solutions—cont'd

REFERENCES

Ganz MB, Boyarsky G, Sterzel RB, et al: Arginine vasopressin enhances pH_i regulation in the presence of HCO_3^- by stimulating three acid–base transport systems. Nature 337:648–651, 1989.

Ganz MB, Perfetto MC, Boron WF: Effects of mitogens and other agents on mesangial cell proliferation, pH and Ca^{2+}. Am J Physiol 259:F269–F278, 1990.

Zhao J, Hogan EM, Bevensee MO, et al: Out-of-equilibrium CO_2/HCO_3^- solutions and their use in characterizing a novel K/HCO_3 cotransporter. Nature 374:636–639, 1995.

Zhao J, Zhou Y, Boron WF: Effect of isolated removal of either basolateral HCO_3^- or basolateral CO_2 on HCO_3^- reabsorption by rabbit S2 proximal tubule. Am J Physiol Renal Physiol 285:F359–F369, 2003.

N28-5 Derivation of the Henderson-Hasselbalch Equation

Contributed by Emile Boulpaep and Walter Boron

As shown in Equation 28-13,

$$CO_2 + H_2O \rightleftarrows H_2CO_3 \rightleftarrows H^+ + HCO_3^-$$
$$CO_2 + H_2O \rightleftarrows H^+ + HCO_3^-$$

We can define a dissociation constant for this pseudoequilibrium:

$$K' = \frac{[H^+][HCO_3^-]}{[CO_2][H_2O]} \quad \textbf{(NE 28-5)}$$

Factoring out $[H_2O]$, we can define an apparent equilibrium constant:

$$K'[H_2O] = K = \frac{[H^+][HCO_3^-]}{[CO_2]} \quad \textbf{(NE 28-6)}$$
$$K = \frac{[H^+][HCO_3^-]}{[CO_2]}$$

The equation immediately above is Equation 28-14 in the text. K at 37°C is $\sim 10^{-6.1}$ M or $10^{-3.1}$ mM. Taking the log (to the base 10) of each side of this equation, and remembering that $\log(a \times b) = \log(a) + \log(b)$, we have

$$\log K = \log[H^+] + \log\frac{[HCO_3^-]}{[CO_2]} \quad \textbf{(NE 28-7)}$$

Remembering that $\log [H^+] \equiv -pH$ and $\log K \equiv -pK$, we may insert these expressions into Equation NE 28-7 and rearrange to obtain

$$pH = pK + \log\frac{[HCO_3^-]}{[CO_2]} \quad \textbf{(NE 28-8)}$$

This expression is the same as Equation 28-15 in the text. Finally, we may express $[CO_2]$ in terms of P_{CO_2}, recalling from Henry's law that $[CO_2] = s \times P_{CO_2}$:

$$pH = pK + \log\frac{[HCO_3^-]}{s \times P_{CO_2}} \quad \textbf{(NE 28-9)}$$

This is the *Henderson-Hasselbalch* equation, a logarithmic restatement of the CO_2/HCO_3^- equilibrium in Equation NE 28-5 above.

N28-6 Derivation of Expressions for Buffering Power in Closed and Open Systems

Contributed by Emile Boulpaep and Walter Boron

How does buffering power, in either a closed or open system, depend on pH?

Closed System

We start with a restatement of Equation 28-8, in which we define buffering power as the amount of strong base that we need to add (per liter of solution) in order to increase the pH by 1 pH unit. In differential form, this definition becomes the following:

$$pH = pK + \log\frac{[HCO_3^-]}{s \times P_{CO_2}}$$

$$\beta \equiv \frac{d[\text{Strong Base Added}]}{d\text{pH}} \qquad \textbf{(NE 28-10)}$$

Second, because the change in the concentration of the unprotonated form of the buffer, $[B^{(n)}]$, is very nearly the same as the amount of strong base added (see Equation 28-7), Equation NE 28-10 becomes

$$\beta \equiv \frac{d[\text{Strong Base}]}{d\text{pH}} \cong \frac{d[B^{(n)}]}{d\text{pH}} \qquad \textbf{(NE 28-11)}$$

The third step is to combine Equation 28-3, reproduced below,

$$K = \frac{[B^{(n)}]\,[H^+]}{[HB^{(n+1)}]} \qquad \textbf{(NE 28-12)}$$

and Equation 28-5, reproduced below,

$$[TB] = [HB^{(n+1)}] + [B^{(n)}] \qquad \textbf{(NE 28-13)}$$

to obtain an expression that describes how $[B^{(n)}]$ depends on the concentration of total buffer, [TB], and $[H^+]$:

$$[B^{(n)}] = [TB]\frac{K}{[H^+] + K} \qquad \textbf{(NE 28-14)}$$

Finally, we obtain the closed-system buffering power by taking the derivative of $[B^{(n)}]$ in Equation NE 28-14 with respect to pH. If we hold [TB] constant while taking this derivative (i.e., if we assume that the buffer can neither enter nor leave the system), we obtain the following expression for β_{closed}:

$$\beta_{closed} = \left(\frac{d[B^{(n)}]}{d\text{pH}}\right)_{[TB]} = 2.3\,[TB]\frac{[H^+]\,K}{([H^+] + K)^2} \qquad \textbf{(NE 28-15)}$$

Open System

How does β_{open} depend on P_{CO_2} and pH? The first two steps of this derivation are the same as for the open system, except that we recognize that, for the CO_2/HCO_3^- buffer pair, $[B^{(n)}]$ is $[HCO_3^-]$:

$$\beta = \frac{d[\text{Strong Base Added}]}{d\text{pH}} = \frac{d[HCO_3^-]}{d\text{pH}} \qquad \textbf{(NE 28-16)}$$

For the open system, the third step is to rearrange the Henderson-Hasselbalch equation (see Equation 28-16, reproduced below),

$$\text{pH} = \text{p}K + \log\frac{[HCO_3^-]}{s \cdot P_{CO_2}} \qquad \textbf{(NE 28-17)}$$

and rearrange it to solve for $[HCO_3^-]$:

$$[HCO_3^-] = s \times P_{CO_2} \times 10^{(\text{pH} - \text{p}K)} \qquad \textbf{(NE 28-18)}$$

If we take the derivative of $[HCO_3^-]$ in the above equation with respect to pH, holding P_{CO_2} constant, the result is β_{open}:

$$\beta_{open} = 2.3 \times s \times P_{CO_2} \times 10^{(\text{pH-p}K)} \qquad \textbf{(NE 28-19)}$$

Because Equation NE 28-18 tells us that everything after "2.3" in the above equation is, in fact, "$[HCO_3^-]$," we obtain the final expression for β_{open}:

$$\beta_{open} = 2.3 \times [HCO_3^-] \qquad \textbf{(NE 28-20)}$$

This is Equation 28-20 in the text.

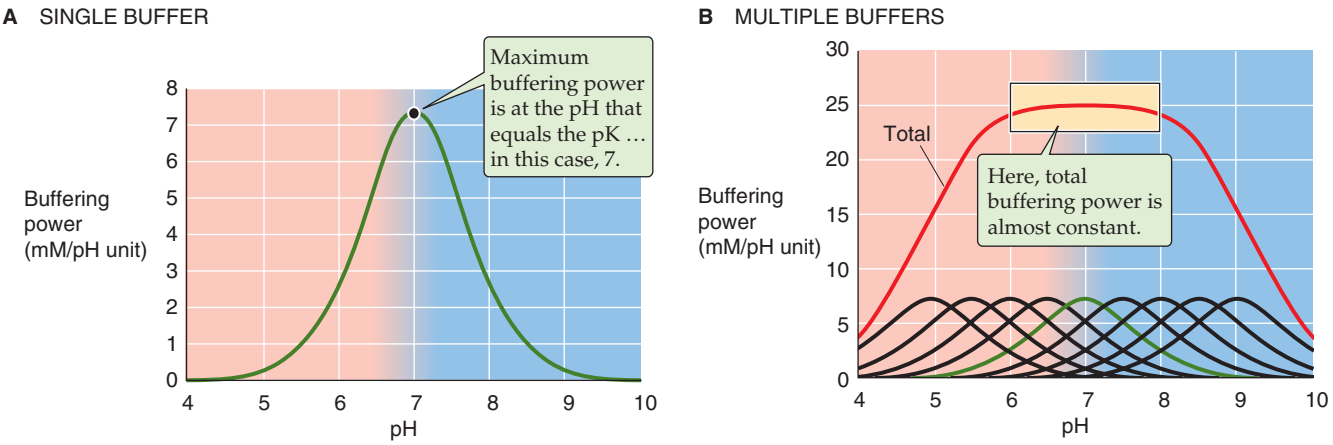

Figure 28-2 Buffering power in a closed system. In **B,** the solution contains nine buffers, each at a concentration of 12.6 mM and with p*K* values evenly spaced 0.5 pH unit apart.

$$\beta_{closed} = 2.3[TB]\frac{[H^+]\cdot K}{([H^+ + K])^2} \qquad \textbf{(28-18)}$$

Two aspects of Equation 28-18 are of interest. First, at a given $[H^+]$, β_{closed} is proportional to [TB]. Second, at a given [TB], β_{closed} has a bell-shaped dependence on pH (green curve in Fig. 28-2*A*). β_{closed} is maximal when $[H^+] = K$ (i.e., when pH = p*K*). Most non-HCO_3^- buffers in biological fluids behave as if they are in a closed system. Although many fluids are actually *mixtures* of several non-HCO_3^- buffers, the total $\beta_{non\text{-}HCO_3^-}$ in such a mixture is the sum of their β_{closed} values, each described by Equation 28-18. The red curve in Figure 28-2*B* shows how total $\beta_{non\text{-}HCO_3^-}$ varies with pH for a solution containing a mixture of nine buffers (including the one described by the green curve), each present at a [TB] of 12.6 mM, with p*K* values evenly spaced at intervals of 0.5 pH unit. In this example, total $\beta_{non\text{-}HCO_3^-}$ is remarkably stable over a broad pH range and has a peak value that is the same as that of whole blood: 25 mM/pH unit. Indeed, whole blood is a complex mixture of many non-HCO_3^- buffers. The most important of these are titratable groups on hemoglobin and, to a far lesser extent, other proteins. Even less important than the "other proteins" are small molecules such as inorganic phosphate. The [TB] values for these many buffers are not identical, and the p*K* values are not evenly spaced. Nevertheless, the buffering power of whole blood is nearly constant near the physiological pH.

The other physiologically important condition under which a buffer can function is in an **open system.** Here, one buffer species (e.g., CO_2) equilibrates between the system and the environment. A laboratory example is a solution containing CO_2 and HCO_3^- in which dissolved CO_2 equilibrates with gaseous CO_2 in the atmosphere (see Fig. 28-1). A physiological example is blood plasma, in which dissolved CO_2 equilibrates with gaseous CO_2 in the alveoli. In either case, $[CO_2]_{dis}$ is fixed during buffering reactions. However, the **total CO_2**—$[CO_2] + [HCO_3^-]$—can vary widely. Because total CO_2 can rise to very high values, CO_2/HCO_3^- in an open system can be an extremely powerful buffer. Consider, for example, a liter of a solution having a pH of 7.4, a P_{CO_2} of 40 mm Hg (1.2 mM CO_2), and an $[HCO_3^-]$ of 24 mM—*but no other buffers* (Fig. 28-3, stage 1). What happens when we add 10 mmol of HCl? Available $[HCO_3^-]$ neutralizes almost all of the added H^+, forming nearly 10 mmol H_2CO_3 and then nearly 10 mmol CO_2 plus nearly 10 mmol H_2O (see Fig. 28-3, stage 2A). The CO_2 that forms does not accumulate, but evolves to the atmosphere so that $[CO_2]_{dis}$ is constant. What is the final pH? If $[CO_2]_{dis}$ remains at 1.2 mM in our open system, and if $[HCO_3^-]$ decreases by almost exactly 10 mM (i.e., the amount of added H^+), from 24 to 14 mM, the Henderson-Hasselbalch equation predicts a fall in pH from 7.40 to 7.17, corresponding to an increase in free $[H^+]$ of

$$\begin{aligned}\Delta[H^+] &= (10^{-7.17} - 10^{-7.40})\ M \\ &= 0.000{,}068\ mM - 0.000{,}040\ mM \\ &= 0.000{,}028\ mM\end{aligned} \qquad \textbf{(28-19)}$$

Even though we have added 10 *milli*moles of HCl to 1 L, $[H^+]$ increased by only 28 *nano*molar (see Fig. 28-3, stage 3*A*). Therefore, the open-system buffer has neutralized 9.999,972 mmol of the added 10 mmol H^+. The buffering provided by CO_2/HCO_3^- in an open system (β_{open}) is so powerful because only depletion of HCO_3^- limits neutralization of H^+. The buildup of CO_2 is not a limiting factor because the atmosphere is an infinite sink for newly produced CO_2.

The opposite acid-base disturbance occurs when we add a strong base such as NaOH. Here, the buffering reactions are just the reverse of those in the previous example. If we add 10 mmol of NaOH to 1 L of solution, almost all added OH^- combines with H^+ derived from CO_2 that enters from the atmosphere (see Fig. 28-3, stage 2B). One HCO_3^- ion forms for each OH^- neutralized. Buffering power in this *open system* is far higher than that in a closed system because CO_2 availability does not limit neutralization of added OH^-. Only the buildup of HCO_3^- limits neutralization of more OH^-. In this example, even though we added 10 *milli*moles NaOH, free $[H^+]$ decreased by only 12 *nano*molars (see Fig. 28-3, stage 3B) as pH rose from 7.40 to 7.55.

Whether CO_2/HCO_3^- neutralizes an acid or a base, the open-system buffering power is N28-6

$$\beta_{open} = 2.3\cdot[HCO_3^-] \qquad \textbf{(28-20)}$$

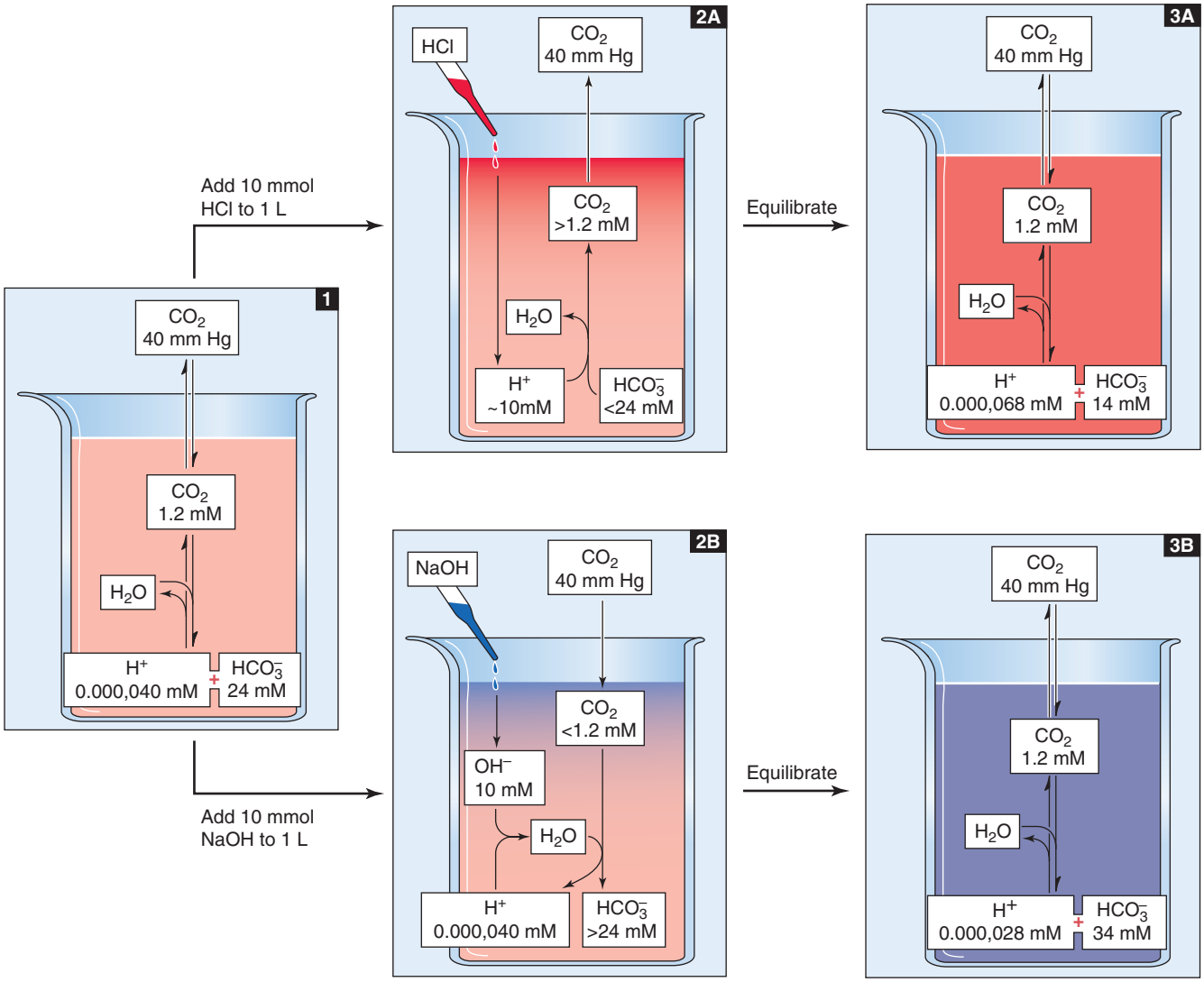

Figure 28-3 Buffering of strong acids and bases by CO_2/HCO_3^- in an open system.

Notice that β_{open} does not have a maximum. Because β_{open} is proportional to $[HCO_3^-]$, β_{open} rises exponentially with pH when P_{CO_2} is fixed (Fig. 28-4, blue curve). In normal arterial blood (i.e., $[HCO_3^-]$ = 24 mM), β_{open} is ~55 mM/pH unit. As we have already noted, the buffering power of all non-HCO_3^- buffers ($\beta_{non\text{-}HCO_3^-}$) in whole blood is ~25 mM/pH unit. Thus, in whole blood, β_{open} represents more than two thirds of the total buffering power. The relative contribution of β_{open} is far more striking in interstitial fluid, which lacks the cellular elements of blood and also has a lower protein concentration.

CO_2/HCO_3^- does not *necessarily* behave as an open-system buffer. In the previous example, we could have added NaOH to a CO_2/HCO_3^- solution in a capped syringe. In such a closed system, not only does accumulation of HCO_3^- limit neutralization of OH^-, but the availability of CO_2 is limiting as well. Indeed, for fluid having the composition of normal arterial blood, the *closed-system* CO_2/HCO_3^- buffering power is only 2.6 mM/pH unit (see Fig. 28-4, black curve), <5% of the β_{open} value of 55 mM/pH unit. You might

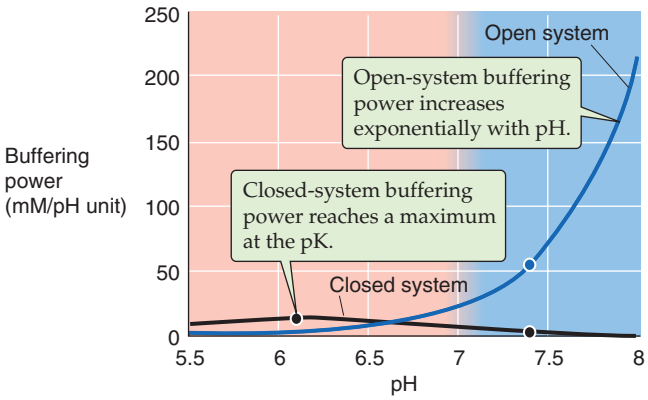

Figure 28-4 Buffering power of the CO_2/HCO_3^- system. At pH 7.4 on the blue curve, the solution has the same composition as does arterial blood plasma: a P_{CO_2} of 40 mm Hg and an $[HCO_3^-]$ of 24 mM. If the system is "open" (i.e., CO_2 equilibrates with atmosphere), β_{open} is ~55 mM/pH unit at pH 7.40 and rises exponentially with pH (see Equation 28-20). If the system is closed, β_{closed} is only ~2.6 mM/pH unit at pH 7.4 and is maximal at the p*K* of the buffer (see Equation 28-18).

think that the only reason the closed-system buffering power was so low in this example is that the pH of 7.4 was 1.3 pH units above the p*K*. However, even if pH were equal to the p*K* of 6.1, the closed-system CO_2/HCO_3^- buffering power in our example would be only ~14 mM/pH unit, about one quarter of the open-system value at pH 7.4. A physiological example in which the CO_2/HCO_3^- system is "poorly open" is **ischemia,** wherein a lack of blood flow minimizes the equilibration of tissue CO_2 with blood CO_2. Thus, ischemic tissues are especially susceptible to large pH shifts.

ACID-BASE CHEMISTRY WHEN CO_2/HCO_3^- IS THE ONLY BUFFER

In this section, we consider buffering by CO_2 and HCO_3^- when these are the *only* buffers present in the solution. We defer to the following section the more complex example in which *both* CO_2/HCO_3^- and non-HCO_3^- buffers are present in the same solution.

In the absence of other buffers, doubling P_{CO_2} causes pH to fall by 0.3 but causes almost no change in $[HCO_3^-]$

Figure 28-5 represents 1 L of a solution with the same CO_2/HCO_3^- composition as arterial blood plasma but no buffers other than CO_2/HCO_3^-. What are the consequences of increasing P_{CO_2} in the gas phase? The resulting increase in $[CO_2]_{dis}$ causes the CO_2/HCO_3^- equilibrium to shift toward formation of H^+ and HCO_3^-. This disturbance is an example of a **CO_2 titration,** because we initiated it by altering P_{CO_2}. More specifically, it is a **respiratory acidosis**—"acidosis" because pH falls, and "respiratory" because pulmonary problems (Table 28-3) are the most common causes of an increase in the P_{CO_2} of arterial blood (see p. 680).

In the absence of non-HCO_3^- buffers, how far pH falls during respiratory acidosis depends on the initial pH and P_{CO_2}, as well as on the final P_{CO_2}. For example, doubling P_{CO_2} from 40 mm Hg (see Fig. 28-5, stage 1) to 80 mm Hg causes $[CO_2]_{dis}$ to double to 2.4 mM (see Fig. 28-5, stage 2A). At this point, the 1-L system is far *out* of equilibrium and can

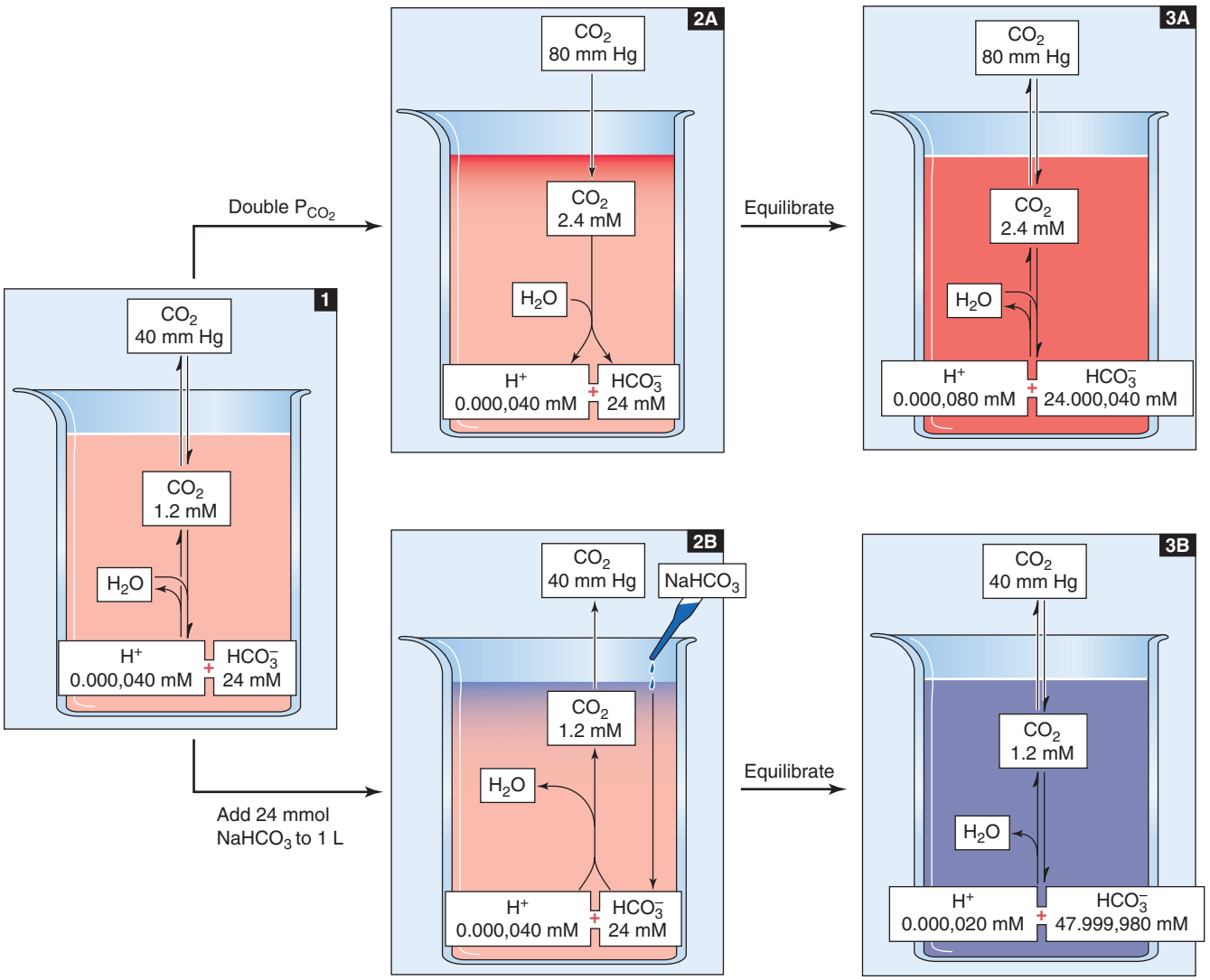

Figure 28-5 Doubling of CO_2 or HCO_3^- concentrations.

TABLE 28-3 The Four Major Acid-Base Disorders

DISORDER	PROXIMATE CAUSE(S)	CLINICAL CAUSES	CHANGES IN ARTERIAL ACID-BASE PARAMETERS
Respiratory acidosis	↑ P_{CO_2}	↓ Alveolar ventilation (e.g., drug overdose) ↓ Lung-diffusing capacity (e.g., pulmonary edema) Ventilation-perfusion mismatch	pH: ↓ $[HCO_3^-]$: ↑ P_{CO_2}: ↑
Respiratory alkalosis	↓ P_{CO_2}	↑ Alveolar ventilation caused by: Hypoxia (e.g., acclimatization to high altitude) Anxiety Aspirin intoxication	pH: ↑ $[HCO_3^-]$: ↓ P_{CO_2}: ↓
Metabolic acidosis	Addition of acids other than CO_2 or H_2CO_3 Removal of alkali (fixed P_{CO_2})	↓ Urinary secretion of H^+ (e.g., renal failure) Ketoacidosis (e.g., diabetes mellitus) Lactic acidosis (e.g., shock) HCO_3^- loss (e.g., severe diarrhea)	pH: ↓ $[HCO_3^-]$: ↓ P_{CO_2}: No change
Metabolic alkalosis	Addition of alkali Removal of acids other than CO_2 or H_2CO_3 (fixed P_{CO_2})	HCO_3^- load (e.g., $NaHCO_3$ therapy) Loss of H^+ (e.g., severe vomiting)	pH: ↑ HCO_3^-: ↑ P_{CO_2}: No change

return to equilibrium only if some CO_2 (X mmol) combines with X H_2O to form X H^+ and X HCO_3^-. Thus, according to Equation 28-14, the following must be true at equilibrium:

$$\underbrace{10^{-6.1}\text{ M}\ \text{ or }\ 10^{-3.1}\text{ mM}}_{K} = \frac{\overbrace{(0.000{,}040\text{ mM}+x)}^{[H^+]}\overbrace{(24\text{ mM}+x)}^{[HCO_3^-]}}{\underbrace{2.4\text{ mM}}_{[CO_2]}} \quad \textbf{(28-21)}$$

Solving this equation for X yields an extremely small value, nearly 40 nmol, or 0.000,040 mmol. X represents the **flux** of CO_2 that passes through the reaction sequence $CO_2 + H_2O \rightarrow H_2CO_3 \rightarrow H^+ + HCO_3^-$ to re-establish the equilibrium. CO_2 from the atmosphere replenishes the CO_2 consumed in this reaction, so that $[CO_2]_{dis}$ remains at 2.4 mM after the new equilibrium is achieved (see Fig. 28-5, stage 3A). The reason that the flux X is so small is that, with no other buffers present, every H^+ formed remains free in solution. Thus, only a minuscule amount of H^+ need be formed before $[H^+]$ nearly doubles from 40 to nearly 80 nM. However, $[HCO_3^-]$ undergoes only a tiny fractional increase, from 24 to 24.000,040 mM. The doubling of the denominator in Equation 28-21 is matched by a doubling of the numerator, nearly all of which is due to the near-doubling of $[H^+]$. The final pH in this example of respiratory acidosis is

$$\text{pH} = -\log(80\text{ nM}) = 7.10 \quad \textbf{(28-22)}$$

Another way of arriving at the same answer is to insert the final values for $[HCO_3^-]$ and P_{CO_2} into the Henderson-Hasselbalch equation:

$$\text{pH} = 6.1 + \log\frac{24.000{,}040\text{ mM}}{(0.03\text{ nM/mm Hg})\cdot(80\text{ mm Hg})} = 7.10 \quad \textbf{(28-23)}$$

The opposite acid-base disturbance, in which P_{CO_2} falls, is **respiratory alkalosis.** In a solution containing no buffers other than CO_2/HCO_3^- reducing P_{CO_2} by half, from 40 to 20 mm Hg, would cause all of the aforementioned reactions to shift in the opposite direction, so that pH would rise by 0.3, from 7.4 to 7.7. We could produce respiratory alkalosis in a beaker by lowering the P_{CO_2} in the gas phase. In humans, hyperventilation (see Table 28-3) lowers alveolar and thus arterial P_{CO_2} (see p. 680).

Thus, in the absence of non-HCO_3^- buffers, doubling $[CO_2]$ causes pH to fall by 0.3, whereas halving $[CO_2]$ causes pH to rise by 0.3 (see Table 28-1). Remember, the log of 2 is 0.3.

In the absence of other buffers, doubling $[HCO_3^-]$ causes pH to rise by 0.3

What would happen if we doubled $[HCO_3^-]$, rather than P_{CO_2}? If we start with 1 L of solution that has the ionic composition of arterial blood (see Fig. 28-5, stage 1), adding 24 mmol of HCO_3^- (e.g., $NaHCO_3$) drives the CO_2/HCO_3^- equilibrium toward CO_2 (see Fig. 28-5, stage 2B). The new equilibrium is achieved when X mmol of HCO_3^- combines with X H^+ to produce X CO_2 and X H_2O. Because the system is *open to* CO_2, the generation of X mmol CO_2 causes no change in $[CO_2]_{dis}$; the newly formed CO_2 simply evolves into the atmosphere. Thus, according to Equation 28-14, the following must be true at equilibrium:

$$\underbrace{10^{-6.1}\text{ M}\ \text{ or }\ 10^{-3.1}\text{ mM}}_{K} = \frac{\overbrace{(0.000{,}040\text{ mM}-x)}^{[H^+]}\overbrace{(48\text{ mM}-x)}^{[HCO_3^-]}}{\underbrace{1.2\text{ mM}}_{\text{Fixed }[CO_2]}} \quad \textbf{(28-24)}$$

Solving this equation yields an X of nearly 0.000,020 mM. Thus, in the absence of other buffers, an initial doubling of $[HCO_3^-]$ from 24 to 48 mM causes $[H^+]$ to fall by nearly half, from 40 to 20 nM. Although $[HCO_3^-]$ also decreases by 20 nM, its fractional change from 48 to 47.999,980 mM is insignificant. The final pH is:

$$\text{pH} = -\log(20\text{ nM}) = 7.70 \quad \textbf{(28-25)}$$

The Henderson-Hasselbalch equation yields the same result:

$$\text{pH} = 6.1 + \log\frac{47.999{,}980\ \text{mM}}{(0.03\ \text{mM/mm Hg})\cdot(40\ \text{mm Hg})} = 7.70 \qquad \textbf{(28-26)}$$

Thus, in the absence of non-HCO_3^- buffers, doubling $[HCO_3^-]$ causes pH to increase by ~0.3. Rather than adding HCO_3^-, we could produce an identical effect by adding the same amount of strong base (e.g., NaOH), as we did in Figure 28-3, stages 2B and 3B, or by *removing* the same amount of strong acid (e.g., HCl). Although the removal of HCl from a solution in a beaker may seem artificial, the removal of gastric HCl from the body occurs during vomiting (see Table 28-3). N28-7 We also could add a *weak* base (e.g., NH_3) or remove any *weak* acid (e.g., lactic acid) other than CO_2 or H_2CO_3. However, to produce the same alkali load, we would have to add/remove more of a *weak* base/acid than for a *strong* base/acid. All of these maneuvers, carried out at a fixed P_{CO_2}, are examples of **metabolic alkalosis**—"alkalosis" because the pH increases, and "metabolic" because derangements in metabolism are common clinical causes.

The opposite acid-base disturbance—in which we remove HCO_3^- or another alkali, or add an acid other than CO_2 or H_2CO_3—is **metabolic acidosis.** If we start with a solution having the ionic composition of arterial blood, removing half of the initial HCO_3^- or removing 12 mM NaOH or adding 12 mM HCl would cause all of the aforementioned reactions to shift in the opposite direction, so that pH would fall by 0.3, from 7.4 to 7.1. Common causes of metabolic acidosis in humans are renal failure and metabolic problems (see Table 28-3).

We saw in Equation 28-26 that the pH of a CO_2/HCO_3^- solution does not depend on $[HCO_3^-]$ or P_{CO_2} per se, but on their ratio. Because it is the kidney that controls $[HCO_3^-]$ in the blood plasma (see Chapter 39), and because it is the lung that controls P_{CO_2} (see Chapter 31), the pH of blood plasma is under the dual control of both organ systems, a concept embodied by a whimsical variant of the Henderson-Hasselbalch equation:

$$\text{pH} = \text{Constant} + \frac{\text{Kidney}}{\text{Lungs}} \qquad \textbf{(28-27)}$$

ACID-BASE CHEMISTRY IN THE PRESENCE OF CO_2/HCO_3^- AND NON-HCO_3^- BUFFERS—THE DAVENPORT DIAGRAM

So far, our discussion has focused on simple systems in which the only pH buffers are either (1) one or more non-HCO_3^- buffers or (2) CO_2/HCO_3^-. Under these circumstances, it is relatively easy to predict the effects of acid-base disturbances. Real biological systems, however, are mixtures of CO_2/HCO_3^- and many non-HCO_3^- buffers. Thus, to understand the effects of respiratory and metabolic acid-base disturbances in a biological system, we must consider multiple competing equilibria—one for CO_2/HCO_3^- (described by Equation 28-16) and one for each of the non-HCO_3^- buffers (each described by its version of Equation 28-5). Obtaining a precise solution to such clinically relevant problems is impossible. One approach is to use a computer to make increasingly more precise approximations of the correct answer. Another, more intuitive approach is to use a graphical method to estimate the final pH. The Davenport diagram is the best such tool.

The Davenport diagram is a graphical tool for interpreting acid-base disturbances in blood

What happens to the pH of blood—a complex mixture that includes many non-HCO_3^- buffers—when P_{CO_2} doubles? We simplify matters by lumping together the actions of all non-HCO_3^- buffers, so that $H^+ + B^{(n)} \rightleftarrows HB^{(n+1)}$ represents the reactions of *all* non-HCO_3^- buffers. When we raise P_{CO_2}, almost all of the newly formed H^+ reacts with $B^{(n)}$ to form $HB^{(n+1)}$ so that the free $[H^+]$ rises only slightly.

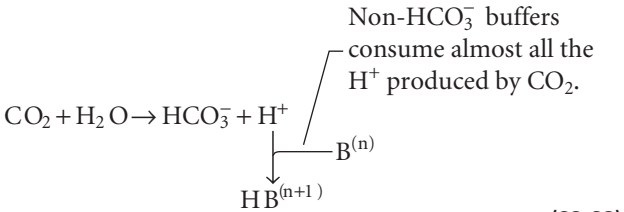

(28-28)

In this simplified approach, the final pH depends on two competing buffer reactions—one involving CO_2/HCO_3^- and the other involving $HB^{(n+1)}/B^{(n)}$. Computing the final pH requires solving two simultaneous equations, one for each buffer reaction.

The CO_2/HCO_3^- Buffer The first of the two equations that we must solve simultaneously is a rearrangement of the Henderson-Hasselbalch equation (see Equation 28-16):

$$[HCO_3^-] = s\cdot P_{CO_2}\cdot 10^{(\text{pH}-\text{p}K_{CO_2})} \qquad \textbf{(28-29)}$$

For a P_{CO_2} of 40 mm Hg, the equation requires that $[HCO_3^-]$ be 24 mM when pH is 7.40—as in normal arterial blood plasma. If pH decreases by 0.3 at this same P_{CO_2}, Equation 28-29 states that $[HCO_3^-]$ must fall by half to 12 mM. Conversely, if pH increases by 0.3, $[HCO_3^-]$ must double to 48 mM. The blue column of Table 28-4 lists the $[HCO_3^-]$ values that Equation 28-29 predicts for various pH

TABLE 28-4 Relationship between HCO_3^- and pH at Three Fixed Levels of P_{CO_2}

	$[HCO_3^-]$ (mM)		
pH	P_{CO_2} = 20 mm Hg	P_{CO_2} = 40 mm Hg	P_{CO_2} = 80 mm Hg
7.1	6 mM	12 mM	24 mM
7.2	8	15	30
7.3	10	19	38
7.4	12	**24**	48
7.5	15	30	60
7.6	19	38	76
7.7	24	48	96

N28-7 Metabolic Alkalosis Caused by Vomiting

Contributed by Walter Boron

Because the stomach secretes HCl into the lumen of the stomach, vomiting necessarily results in a net loss of HCl, N28-9 and this by itself causes some degree of metabolic alkalosis (see p. 635). In addition, the loss of Cl^- leads to volume contraction, that is, a decrease in **effective circulating volume** (see pp. 554–555). The body's multipronged response to this volume contraction (see p. 838) includes a stimulation of the renin-angiotensin-aldosterone axis, the end point of which is increased retention of NaCl and the osmotically obligated H_2O. However, at the level of the renal proximal tubule, the increased levels of systemic [angiotensin II] lead not only to an increase in NaCl reabsorption, but also to an increase in $NaHCO_3$ reabsorption. Moreover, at the level of the distal nephron, the increased levels of aldosterone lead not only to an increase in NaCl reabsorption, but also to an increase in $NaHCO_3$ reabsorption. The result is that the hormonal stimuli that represent the appropriate response to volume depletion lead, as a side effect, to a metabolic alkalosis. The proper treatment of this **contraction alkalosis** is not to infuse the patient with $NaHCO_3$, but rather to replenish the lost volume by delivering "normal saline" intravenously. With effective circulating volume returned to normal, the stimulus to the renin-angiotensin-aldosterone axis is removed, and the acid-base disturbance resolves.

It is interesting to note that although volume depletion causes the kidney not only to retain NaCl but also to retain $NaHCO_3$ inappropriately, the converse is not true. That is, respiratory or metabolic acidosis cause the kidney to retain $NaHCO_3$ but to decrease the reabsorption of NaCl, so as to maintain a constant effective circulating volume.

What this all teaches us is that the defense of effective circulating volume trumps everything (including acid-base homeostasis). However, the body's mechanisms for regulating acid-base balance are far more sophisticated than those for regulating effective circulating volume. Thus, the response to acidosis or alkalosis is precise and appropriate—and does not involve inappropriate changes in effective circulating volume that would otherwise lead to hyper- or hypotension!

N28-9 Equivalency of Adding HCO_3^-, Adding OH^-, and Removing H^+

Contributed by Walter Boron

Imagine that we start with 1 L of an aqueous solution at 37°C. This solution mimics blood plasma, 5% CO_2/24 mM HCO_3^- at pH 7.4, and the system is "open" for CO_2 (i.e., CO_2 can freely enter and leave the aqueous solution so as to keep [CO_2] constant). Moreover, this solution contains a non-HCO_3^- buffer ($HB^{(n+1)} \rightleftarrows H^+ + B^{(n)}$) with a buffering power of 25 mM/pH unit.

Add $NaHCO_3$

If we were to add 1 mmol of $NaHCO_3$ to this 1 L of solution, then [HCO_3^-] would instantly increase by 1 mM. Of course, over time, subsequent reactions cause [HCO_3^-] to gradually fall as the added HCO_3^- equilibrates with the pre-existing CO_2/HCO_3^- buffer according to the overall reactions:

$$HCO_3^- + H^+ \rightarrow CO_2 + H_2O \qquad \textbf{(NE 28-25)}$$

Furthermore, because the consumption of HCO_3^- goes hand in hand with the consumption of H^+, the pH will gradually rise, which in turn upsets the equilibrium of non-HCO_3^- buffers:

$$HB^{(n+1)} \rightarrow H^+ + B^{(n)} \qquad \textbf{(NE 28-26)}$$

Thus, the rise in pH causes the $HB^{(n+1)}/B^{(n)}$ equilibrium to shift to the right, thereby increasing [$B^{(n)}$]. As a result, the final Δ[HCO_3^-] would be <1 mM. However, the changes in [HCO_3^-] and [$B^{(n)}$] would sum to very nearly 1 mM (i.e., the amount of $NaHCO_3$ originally added):

$$\Delta[HCO_3^-] + \Delta[B^{(n)}] \cong 1\ \text{mM} \qquad \textbf{(NE 28-27)}$$

The reason why we use "approximately equal" in the above equation is that a tiny amount of the added HCO_3^- causes the pH to rise (i.e., it is not reflected in the $\Delta[B^{(n)}]$).

Add NaOH

Imagine that instead of adding $NaHCO_3$, we add 1 mmol of NaOH to our 1 L of solution. We can *imagine* that virtually all of the added OH^- would react with the CO_2 to form an equivalent amount of HCO_3^-:

$$OH^- + CO_2 \rightarrow HCO_3^- \qquad \textbf{(NE 28-28)}$$

(Note: this reaction is equivalent to $CO_2 + H_2O \rightarrow HCO_3^- + H^+$.) Thus, [$HCO_3^-$] would rise by very nearly 1 mM. The reason we say "very nearly" is that a tiny fraction of the added OH^- would equilibrate with H^+ and H_2O, causing pH to rise:

$$OH^- + H^+ \rightarrow H_2O \qquad \textbf{(NE 28-29)}$$

This consumption of OH^- would cause pH to rise, which in turn would cause the $HB^{(n+1)}/B^{(n)}$ equilibrium to shift to the right:

$$HB^{(n+1)} \rightleftarrows H^+ + B^{(n)} \qquad \textbf{(NE 28-30)}$$

As a result [$B^{(n)}$] would rise by a tiny amount. At the same time, however, the reaction $CO_2 + H_2O \rightleftarrows HCO_3^- + H^+$ is out of equilibrium because the HCO_3^- that we formed in Equation NE 28-28 yields an [HCO_3^-] far too high for the prevailing [H^+]. Thus, Equation NE 28-28 would partially reverse, releasing more OH^- to react with H^+, and leading to the formation of still more $B^{(n)}$. This reversal of Equation NE 28-28 (the secondary fall in [HCO_3^-]) would continue until eventually the reactions in both Equation NE 28-28 and Equation NE 28-30 are in equilibrium. This process is illustrated by the panels on the right side of Figure 28-7. As a result, the final Δ[HCO_3^-] would be less than the ~1 mM that we predicted in Equation NE 28-28. However, the changes in [HCO_3^-]

Continued

N28-9 Equivalency of Adding HCO_3^-, Adding OH^-, and Removing H^+—cont'd

and $[B^{(n)}]$ would sum to very nearly 1 mM (i.e., the amount of NaOH added):

$$\Delta[HCO_3^-] + \Delta[B^{(n)}] \cong 1 \text{ mM} \quad \textbf{(NE 28-31)}$$

In fact, the values of $\Delta[HCO_3^-]$ and $\Delta[B^{(n)}]$ in Equation NE 28-31 (i.e., the example in which we added 1 mmol NaOH) are precisely the same as in Equation NE 28-27 (i.e., the example in which we added 1 mmol $NaHCO_3$).

Two provisos here. First, the reaction in Equation NE 28-28 would be very slow in the absence of added **carbonic anhydrase.** N18-3 Nevertheless, even in the absence of carbonic anhydrase, this reaction would eventually come to equilibrium, and we could imagine that $[HCO_3^-]$ would eventually rise by very nearly 1 mM. Second, in this thought experiment, we are "imagining" that the added OH^- initially reacts only with CO_2 to form ~1 mM HCO_3^-, and that some of this HCO_3^- then dissociates to yield some CO_2 and OH^-. In fact, a sizeable amount of the OH^- that we originally added will also react instantly with H^+ (according to Equation NE 28-29), in turn leading to the formation of $B^{(n)}$ in Equation NE 28-30.

Remove HCl

Finally, imagine that we magically remove 1 mmol of HCl from a liter of our CO_2/HCO_3^- solution. In real life, we could remove this H^+ either by consuming it in a chemical (or biochemical) reaction or by transporting it out of some biological compartment (e.g., the cytosol). We could *imagine* that the HCl that we remove causes the CO_2/HCO_3^- equilibrium to shift, thereby causing $[HCO_3^-]$ to rise by very nearly 1 mM:

$$CO_2 + H_2O \rightarrow H^+ + HCO_3^- \quad \textbf{(NE 28-32)}$$

The consumed CO_2 would come from the atmosphere. A small amount of the H^+ that we removed would lower pH:

$$H_2O \rightarrow OH^- + H^+ \quad \textbf{(NE 28-33)}$$

However, the reaction in Equation NE 28-32 would be badly out of equilibrium because the rise in $[HCO_3^-]$ would be out of proportion to the fall in $[H^+]$. Thus, the reaction in Equation NE 28-32 would begin to reverse, consuming some of the ~1 mM HCO_3^- that we initially formed. Moreover, the $HB^{(n+1)}/B^{(n)}$ reaction would also be out of equilibrium because $[H^+]$ has fallen without any change in $[B^{(n)}]$ or $[HB^{(n+1)}]$. As a result, the following will occur:

$$HB^{(n+1)} \rightarrow H^+ + B^{(n)} \quad \textbf{(NE 28-34)}$$

In fact, the reaction in Equation NE 28-32 would continue to reverse, releasing some HCO_3^- as well as an equal amount of H^+ for consumption in Equation NE 28-34. Eventually, the reactions in Equations NE 28-32 through NE 28-34 would be in equilibrium. At this point,

$$\Delta[HCO_3^-] + \Delta[B^{(n)}] \cong 1 \text{ mM} \quad \textbf{(NE 28-35)}$$

In fact, the values of $\Delta[HCO_3^-]$ and $\Delta[B^{(n)}]$ in Equation NE 28-35 (i.e., this example in which we removed 1 mmol HCl) are precisely the same as in Equation NE 28-27 (i.e., the example in which we added 1 mmol $NaHCO_3$) and in Equation NE 28-31 (i.e., the example in which we added 1 mmol NaOH).

Summary

Thus, regardless of whether we add 1 mmol of $NaHCO_3$, add 1 mmol of NaOH, or remove 1 mmol of HCl … in the end, the result is the same. The CO_2/HCO_3^- and the $HB^{(n+1)}/B^{(n)}$ buffer systems will both wind up being in equilibrium, and in each example, $[HCO_3^-]$ will increase by the same amount, $[B^{(n)}]$ will increase by the same amount, and pH will increase by the same amount.

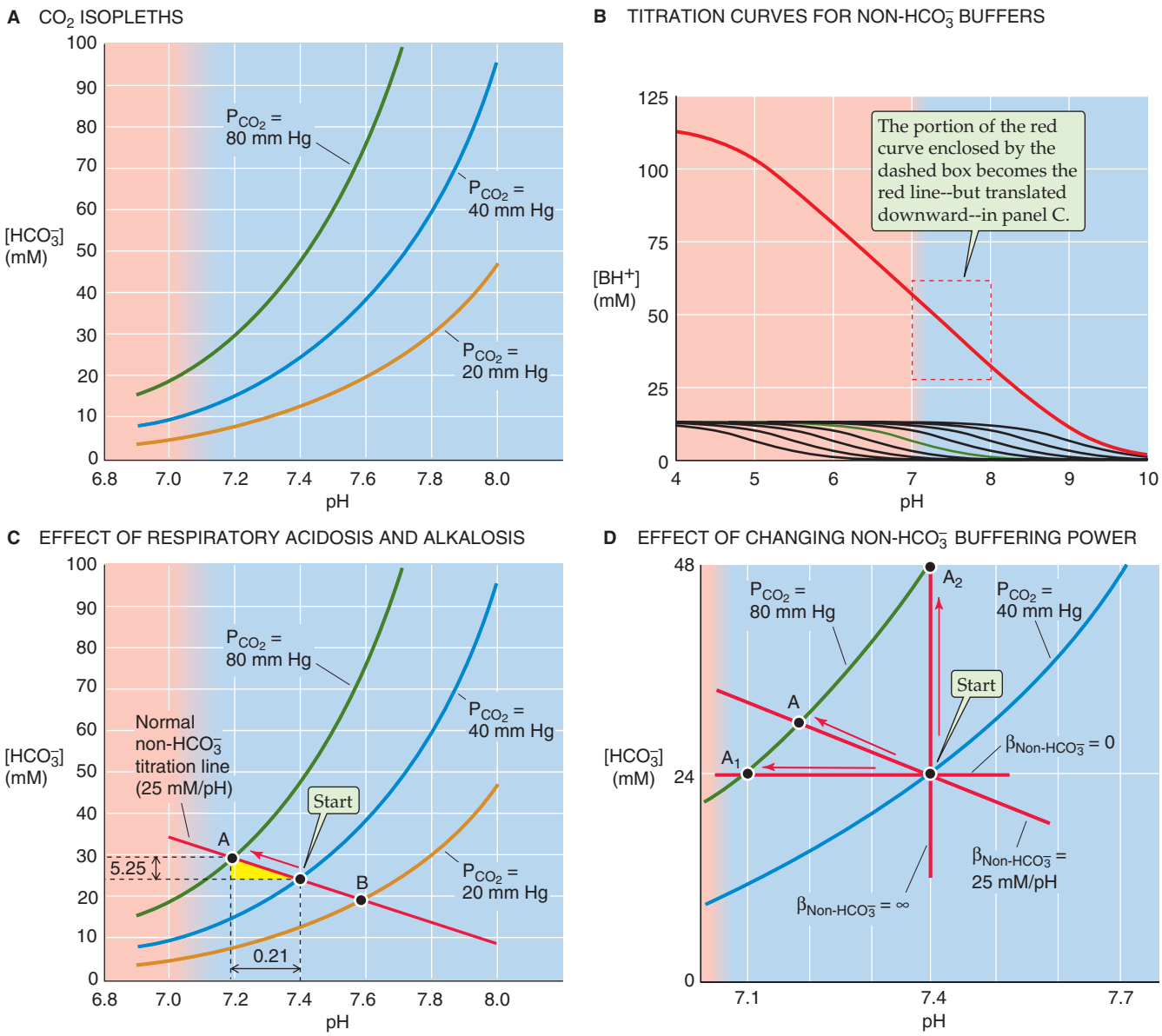

Figure 28-6 Davenport diagram. In **A,** the three isopleths are CO_2 titration curves. In **B,** the solution contains nine buffers, each at a concentration of 12.6 mM and with p*K* values evenly spaced 0.5 pH unit apart, as in Figure 28-2*B*. In **C,** the red arrow represents the transition from a normal acid-base status for blood ("Start") to respiratory acidosis (point A) produced by raising P_{CO_2} to 80 mm Hg. Point B represents respiratory alkalosis produced by lowering P_{CO_2} to 20 mm Hg. In **D,** the labeled points represent the results of respiratory acidosis when $\beta_{non\text{-}HCO_3^-}$ is zero (point A_1), 25 mM/pH (point A), and infinity (point A_2).

values when P_{CO_2} is 40 mm Hg. Plotting these $[HCO_3^-]$ values against pH yields the blue curve labeled "P_{CO_2} = 40 mm Hg" in Figure 28-6*A*. This curve, which is known as a CO_2 isobar or **isopleth** (from the Greek *isos* [equal] + *plethein* [to be full]) represents all possible combinations of HCO_3^-] and pH at a P_{CO_2} of 40 mm Hg. Table 28-4 also summarizes $[HCO_3^-]$ values prevailing at P_{CO_2} values of 20 and 80 mm Hg. Note that at a P_{CO_2} of 20 (orange column), representing respiratory alkalosis, $[HCO_3^-]$ values are half those for a P_{CO_2} of 40 at the same pH. At a P_{CO_2} of 80 (green column), representing respiratory acidosis, $[HCO_3^-]$ values are twice those at a P_{CO_2} of 40. Each of the isopleths in Figure 28-6*A* rises exponentially with pH. The slope of each isopleth also rises exponentially with pH and represents β_{open} for CO_2/HCO_3^-. At a particular pH, an isopleth representing a higher P_{CO_2} (i.e., a higher $[HCO_3^-]$) has a steeper slope, as Equation 28-20 predicts.

Non-HCO_3^- Buffers The second of the two equations that we must solve simultaneously describes the lumped reaction of all non-HCO_3^- buffers. To understand the origin of this equation, we begin with the green curve (surrounded by black curves) in Figure 28-6*B*, the **titration curve** of a single non-HCO_3^- buffer with a p*K* of 7 and total buffer concentration of 12.6 mM (as for the green curve in Fig. 28-2*B*). At a pH of 10, $[HB^{(n+1)}]$ for this single buffer is extremely low

because almost all of the "B" is in the form $B^{(n)}$. As we lower pH by successively adding small amounts of HCl, $[HB^{(n+1)}]$ gradually rises—most steeply when pH equals p*K*. Indeed, at any pH, the slope of this curve is the negative of β for this single buffer. The black curves in Figure 28-6*B* are the titration curves for eight other buffers, each present at a [TB] of 12.6 mM, with p*K* values evenly spaced at intervals of 0.5 pH unit on either side of 7. The red curve in Figure 28-6*B* is the sum of the titration curves for all nine buffers. N28-8 Its slope—the negative of the total buffering power of all nine buffers—is remarkably constant over a broad pH range. (The red curve in Figure 28-2*B* shows how β, the slope of the red curve here in Figure 28-6*B*, varies with pH.) The red curve in Figure 28-6*B* represents the second of the two equations that we must solve simultaneously.

Solving the Problem Figure 28-6*C* is a Davenport diagram, a combination of the three CO_2 isopleths in Figure 28-6*A* and the linear part of the red non-HCO_3^- titration curve in Figure 28-6*B*. The red non-HCO_3^- titration line (representing $\beta_{non\text{-}HCO_3^-}$ for whole blood, 25 mM/pH unit) intersects with the CO_2 isopleth for a P_{CO_2} of 40 at the point labeled "Start," which represents the initial conditions for arterial blood. At this intersection, both CO_2/HCO_3^- and non-HCO_3^- buffers are simultaneously in equilibrium.

We are now in a position to answer the question raised at the beginning of this section: What will be the final pH when we increase the P_{CO_2} of whole blood from 40 to 80 mm Hg? The final equilibrium conditions for this case of *respiratory acidosis* must be described by a point that lies simultaneously on the red non-HCO_3^- titration line and the green isopleth for 80 mm Hg. Obtaining the answer using the Davenport diagram requires a three-step process:

Step 1: Identify the point at the intersection of the initial P_{CO_2} isopleth and the initial non-HCO_3^- titration line (see Fig. 28-6*C*, "Start").
Step 2: Identify the isopleth describing the *final* P_{CO_2} (80 mm Hg in this case).
Step 3: Follow the non-HCO_3^- titration line to its intersection with the final P_{CO_2} isopleth. In Figure 28-6*C*, this intersection occurs at point A, which corresponds to a pH of 7.19 and an $[HCO_3^-]$ of 29.25 mM.

As discussed above, in the *absence* of non-HCO_3^- buffers, this same doubling of P_{CO_2} causes a larger pH decrease, from 7.4 to 7.1.

By following three similar steps, we can use the Davenport diagram to predict the final pH and $[HCO_3^-]$ under conditions of a *respiratory alkalosis*. For example, what would be the effect of decreasing P_{CO_2} by half, from 40 to 20 mm Hg? In Figure 28-6*C* follow the red non-HCO_3^- titration line from "Start" to its intersection with the orange isopleth for a P_{CO_2} of 20 mm Hg (point B), which corresponds to a pH of 7.60 and an $[HCO_3^-]$ of 19 mM. If the solution had *not* contained non-HCO_3^- buffers, halving the P_{CO_2} would have caused a larger pH increase, from 7.4 to 7.7.

The amount of HCO_3^- formed or consumed during "respiratory" acid-base disturbances increases with $\beta_{non\text{-}HCO_3^-}$

Although it is reasonable to focus on CO_2 during respiratory acid-base disturbances, it would be wrong to assume that $[HCO_3^-]$ is constant. For example, in Figure 28-6*C*, where $\beta_{non\text{-}HCO_3^-}$ is 25 mM/pH unit, increasing P_{CO_2} from 40 to 80 mm Hg causes $[HCO_3^-]$ to increase from 24 to 29.25 mM. Thus, in each liter of solution, 5.25 mmol CO_2 combines with 5.25 mmol H_2O to form 5.25 mmol HCO_3^- (which we see as the $\Delta[HCO_3^-]$ value between "Start" and point A) and 5.25 mmol H^+. Nearly all of this H^+ disappears as nearly 5.25 mmol of the deprotonated non-HCO_3^- buffers ($B^{(n)}$) consumes H^+ to form nearly 5.25 mmol of their conjugate weak acids ($HB^{(n+1)}$). Thus, the flux through the reaction sequence in Equation 28-28 is nearly 5.25 mmol for each liter of solution.

$$CO_2 + H_2O \xrightarrow{5.25\,mM} HCO_3^- + H^+ \quad (28\text{-}30)$$
$$\sim 5.25\,mM \downarrow \quad B^{(n)} \rightarrow HB^{(n+1)}$$

Thus, the non-HCO_3^- buffers drive the conversion of CO_2 to HCO_3^-. These buffers minimize the increase in free $[H^+]$ that a given flux of CO_2 can produce. Thus, with a high $\beta_{non\text{-}HCO_3^-}$, a large amount of CO_2 must "flux" through Equation 28-30 before the free concentrations of HCO_3^- and H^+ rise sufficiently to satisfy the CO_2/HCO_3^- equilibrium (see Equation 28-14).

$\beta_{non\text{-}HCO_3^-}$ varies with the hemoglobin content of blood. Thus, patients with anemia have a low $\beta_{non\text{-}HCO_3^-}$, whereas patients with polycythemia have a high $\beta_{non\text{-}HCO_3^-}$.

Figure 28-6*D* illustrates the importance of $\beta_{non\text{-}HCO_3^-}$. If $\beta_{non\text{-}HCO_3^-}$ is zero, the non-HCO_3^- titration line is horizontal, and doubling P_{CO_2} from 40 to 80 mm Hg does not change $[HCO_3^-]$ significantly (see Fig. 28-6*D*, point A_1); this verifies our earlier conclusion (see Fig. 28-5, stage 3A). Simultaneously, pH falls by 0.3, which corresponds to a near-doubling of $[H^+]$. Thus, doubling $[CO_2]$ leads to a doubling of the product $[HCO_3^-][H^+]$, so that the ratio $[HCO_3^-][H^+]/[CO_2]$—the equilibrium constant, *K*—is unchanged (Table 28-5, top row). Figure 28-6*D* also shows what happens if $\beta_{non\text{-}HCO_3^-}$

TABLE 28-5 Relationship between $\beta_{non\text{-}HCO_3^-}$ and the Amount of HCO_3^- Formed in Response to a Doubling of P_{CO_2}

NON-HCO_3^- BUFFERING POWER	ΔpH	HCO_3^- FORMED (mM)	FRACTIONAL $\Delta[H^+]$	FRACTIONAL $\Delta[HCO_3^-]$	FRACTIONAL $\Delta[HCO_3^-] \times \Delta[H^+]$
0	–0.30	0.000,040	1.999,997	1.000,002	2.00
25	–0.21	5.25	1.71	1.17	2.00
∞	0	24.0	1.00	2.00	2.00

N28-8 Davenport Diagram—Constructing the Non-HCO_3^- Buffer Line

Contributed by Emile Boulpaep and Walter Boron

The **non-HCO_3^- buffer line** (the red line in Fig. 28-6*B, C*) describes the buffering power of *all buffers other than CO_2/HCO_3^-* ($\beta_{non\text{-}HCO_3^-}$). In whole blood—here we refer to the line as the **blood buffer line**—hundreds of buffer groups may contribute to the overall non-HCO_3^- buffering power. Each of these buffer groups has its own p*K* and concentration, and thus its own bell-shaped curve—like the nine small curves in Figure 28-2*B*—describing the pH dependence of its buffering power. Each of these buffer groups also has its own titration curve, as shown in Fig. 28-6*B,* and the sum of these titration curves (the red curve in this figure) is the combined titration curve of these buffers (i.e., $\beta_{non\text{-}HCO_3^-}$). Notice that this red curve is nearly a straight line over the physiological pH range. In other words, in the physiological range, the slope of the red line is nearly constant, which is another way of stating that the non-HCO_3^- buffering power is nearly constant over this pH range—as illustrated in Figure 28-2*B*.

We already know from Equation 28-8 (reproduced below as Equation NE 28-21) that we can define buffering power in terms of the amount of strong acid added to the solution:

$$\beta_{Non\text{-}HCO_3^-} \equiv -\frac{\overbrace{\Delta[\text{Strong Acid}]}^{\text{moles/L}}}{\Delta pH} \qquad \textbf{(NE 28-21)}$$

From the perspective of the non-HCO_3^- buffers that are at work during respiratory acidosis, Δ[strong acid] is the H^+ formed from CO_2 and H_2O as a result of the increase in P_{CO_2} (see arrow from "Start" to point A in Fig. 28-6*C*). Because respiratory acidosis produces HCO_3^- and H^+ in a 1:1 ratio, the amount of HCO_3^- formed during respiratory acidosis—that is $[HCO_3^-]_{final} - [HCO_3^-]_{initial} = \Delta[HCO_3^-]$—is the same as the amount of H^+ added (Δ[strong acid]). Thus, we can replace Δ[strong acid] in Equation NE 28-21 with $\Delta[HCO_3^-]$ and therefore somewhat paradoxically express the non-HCO_3^- buffering power in terms of $[HCO_3^-]$:

$$\beta_{Non\text{-}HCO_3^-} \equiv -\frac{\Delta[\text{Strong Acid}]}{\Delta pH} \cong -\frac{\Delta[HCO_3^-]}{\Delta pH} = \frac{[HCO_3^-]_{init} - [HCO_3^-]}{pH - pH_{init}} \qquad \textbf{(NE 28-22)}$$

$[HCO_3^-]_{init}$ and pH_{init} represent initial values (before increasing P_{CO_2}—that is, the point labeled "Start" in Fig. 28-6*C*), and $[HCO_3^-]$ and pH represent *final* values (after increasing P_{CO_2}—that is, point A in Fig. 28-6*C*). The equation describing the non-HCO_3^- buffer line is simply a rearrangement of Equation NE 28-22:

$$[HCO_3^-] = [HCO_3^-]_{init} - \beta_{Non\text{-}HCO_3^-}(pH - pH_{init}) \qquad \textbf{(NE 28-23)}$$

This equation describes a line whose slope is *negative* $\beta_{non\text{-}HCO_3^-}$. For whole blood, $\beta_{non\text{-}HCO_3^-}$ is 25 mM/pH unit, so that the slope of the line is –25 mM/pH unit in Figure 28-6*C*. Note that because we assumed that the buffering power of the non-HCO_3^- buffers is constant over the pH range of interest, and because this buffering power is represented by the *slope* of the non-HCO_3^- buffer curve in Figure 28-6*C,* the function describing this buffering power must be a straight line (i.e., a function with a constant slope).

We are now in a position to understand why, in Figure 28-6*C,* the non-HCO_3^- buffer line (see Equation NE 28-23) shares the same y-axis as the CO_2 isopleth (e.g., the blue curve in Fig. 28-6*C*), which is described by Equation 28-29, reproduced here:

$$[HCO_3^-] = s \times P_{CO_2} \times 10^{(pH - pK_{CO_2})} \qquad \textbf{(NE 28-24)}$$

In both the case of the line describing the non-HCO_3^- buffering power (see Equation NE 28-23) and the exponential curve describing the open-system CO_2 buffering power (see Equation NE 28-24), the dependent variable is $[HCO_3^-]$.

The non-HCO_3^- buffer line passes through the point describing the initial conditions (pH_{init}, $[HCO_3^-]_{init}$). In Figure 28-6*C,* pH_{init} is 7.40 and $[HCO_3^-]_{init}$ is 24 mM, as indicated by the point labeled "Start." Because these initial conditions for the non-HCO_3^- buffers can change, we will see below in the text that the non-HCO_3^- buffer line can translate up and down on the Davenport diagram in metabolic alkalosis and metabolic acidosis. However, as long as $\beta_{non\text{-}HCO_3^-}$ is constant, the slope of the line is always the same.

has the normal value of 25 mM/pH unit. Here, point A is the same as point A in Figure 28-6*C*, and it shows that $[HCO_3^-]$ increases by 5.25 mM, or 17% (see Table 28-5, middle row). Finally, if $\beta_{non\text{-}HCO_3^-}$ were ∞, the non-HCO_3^- titration line would be vertical, and doubling P_{CO_2} would not change pH at all (point A_2 in Fig. 28-6*D*). In this case, $[HCO_3^-]$ would double, so that the doubling of the product $[HCO_3^-][H^+]$ would match the doubling of P_{CO_2} (see Table 28-5, bottom row).

Adding or removing an acid or base—at a constant P_{CO_2}—produces a "metabolic" acid-base disturbance

Above, we examined the effect of adding HCl in the *absence* of other buffers (see Fig. 28-3). Predicting the pH change for such an acid-base disturbance was straightforward because the titration of HCO_3^- to CO_2 consumed all buffered H^+. The situation is more complex when the solution also contains non-HCO_3^- buffers (Fig. 28-7, stage 1). When we add 10 mmol of HCl to 1 L of solution, the open-system CO_2/HCO_3^- buffer pair neutralizes most of the added H^+, non-HCO_3^- buffers handle some, and a minute amount of added H^+ remains free and lowers pH (see Fig. 28-7, stage 2A). Because the system is open, the CO_2 formed during buffering of the added H^+ escapes to the atmosphere. If this buffering reaction were occurring in the blood, the newly formed CO_2 would escape first into the alveolar air, and then into the atmosphere.

How much of the added H^+ (Δ[strong acid] = 10 mM) follows each of the three pathways in this example of *metabolic acidosis*? Answering this question requires dealing with two competing equilibria, the CO_2/HCO_3^- and the non-HCO_3^- buffering reactions. As for respiratory acid-base disturbances, we cannot precisely solve the equations governing metabolic acid-base disturbances. However, we can use the Davenport diagram on the left of Figure 28-7 to obtain a graphical estimate of the final pH and $[HCO_3^-]$ through a four-step process:

Step 1: Identify the point describing the initial conditions (see Fig. 28-7, "Start" in graph on left).

Step 2: Following the black arrow labeled "2," move downward (in the direction of decreased $[HCO_3^-]$) by 10 mM—the concentration of added H^+—to the point labeled with an asterisk. In this maneuver, we assume that the reaction $HCO_3^- + H^+ \rightarrow CO_2 + H_2O$ has initially consumed *all* of the added H^+. Of course, if this were true, the CO_2/HCO_3^- reaction would be far out of equilibrium and the pH would not have changed at all. Also, the non-HCO_3^- buffers would not have had a chance to participate in the buffering of H^+.

Step 3: Through the asterisk, draw a line (see Fig. 28-7, black line in left graph) that is parallel to the non-HCO_3^- titration line.

Step 4: Following the black arrow labeled "4," move to the intersection of the new black line and the original P_{CO_2} isopleth. This intersection occurs at point C, which corresponds to a pH of 7.26 and an $[HCO_3^-]$ of 17.4 mM. This maneuver tracks the reaction $CO_2 + H_2O \rightarrow HCO_3^- + H^+$. Non-$HCO_3^-$ buffers consume nearly all of this H^+ in the reaction $H^+ + B^{(n)} \rightarrow HB^{(n+1)}$. As a result, $[HCO_3^-]$, $[H^+]$, and $[HB^{(n+1)}]$ all rise and the system equilibrates.

As a shortcut, we could bypass the two black arrows and simply follow the red arrow along the CO_2 isopleth from "Start" to point C.

We now can return to the question of how much of the added H^+ follows each of the three pathways in Figure 28-7, stage 2A. Because $[HCO_3^-]$ decreased by 24 − 17.4 = 6.6 mM, the amount of H^+ buffered by CO_2/HCO_3^- must have been 6.6 mmol in each liter. Almost all of the remaining H^+ that we added, nearly 3.4 mmol, must have been buffered by non-HCO_3^- buffers. A tiny amount of the added H^+, ~0.000,015 mmol, must have remained unbuffered and was responsible for decreasing pH from 7.40 to 7.26 (see Fig. 28-7, stage 3A).

Figure 28-7 also shows what would happen if we added 10 mmol of a strong base such as NaOH to our 1-L solution. The open-system CO_2/HCO_3^- buffer pair neutralizes most of the added OH^-, non-HCO_3^- buffers handle some, and a minute amount of added OH^- remains unbuffered, thus raising pH (see Fig. 28-7, stage 2B). The Davenport diagram on the right of Figure 28-7 shows how much of the added OH^- follows each of the three pathways in this example of *metabolic alkalosis*. The approach is similar to the one we used above for metabolic acidosis, except that in this case, we generate a new black line that is displaced 10 mM *above* the non-HCO_3^- titration line. We follow the P_{CO_2} isopleth to its intersection with this black line at point D, which corresponds to a final pH of 7.51 and an $[HCO_3^-]$ of 31.1 mM. Thus, $[HCO_3^-]$ rose by 31.1 − 24.0 = 7.1 mM. This is the amount of added OH^- that CO_2/HCO_3^- buffered. Non-HCO_3^- buffers must have buffered almost all of the remaining OH^- that we added, ~2.9 mmol in each liter. The unbuffered OH^-, which was responsible for the pH increase, must have been in the nanomolar range (see Fig. 28-7, stage 3B, and Box 28-1).

During metabolic disturbances, CO_2/HCO_3^- makes a greater contribution to total buffering when pH and P_{CO_2} are high and when $\beta_{non\text{-}HCO_3^-}$ is low

In Figure 28-7, CO_2/HCO_3^- neutralized 7.1 mmol of the 10 mmol of OH^- added to 1 L (ΔpH = +0.11) but only

BOX 28-1 Strong Ion Difference

Some clinicians assess acid-base disorders in terms of a virtual parameter termed **strong-ion difference (SID).** Unlike weak acids and bases, the so-called strong cations and strong anions are fully dissociated at physiological pH. In blood,

$$SID = [Na^+] + [K^+] + [Ca^{2+}] + [Mg^{2+}] - [Cl^-]$$

Three major limitations to the SID approach are that (1) proteins and physiological processes generally depend on pH, not SID; (2) cells and the body closely regulate pH but have no known mechanism for directly sensing or regulating SID; and (3) SID neither is uniquely related to pH nor has a causal role in changing pH. Because the SID approach provides no new mechanistic insight, we focus on the classical pH/buffer approach.

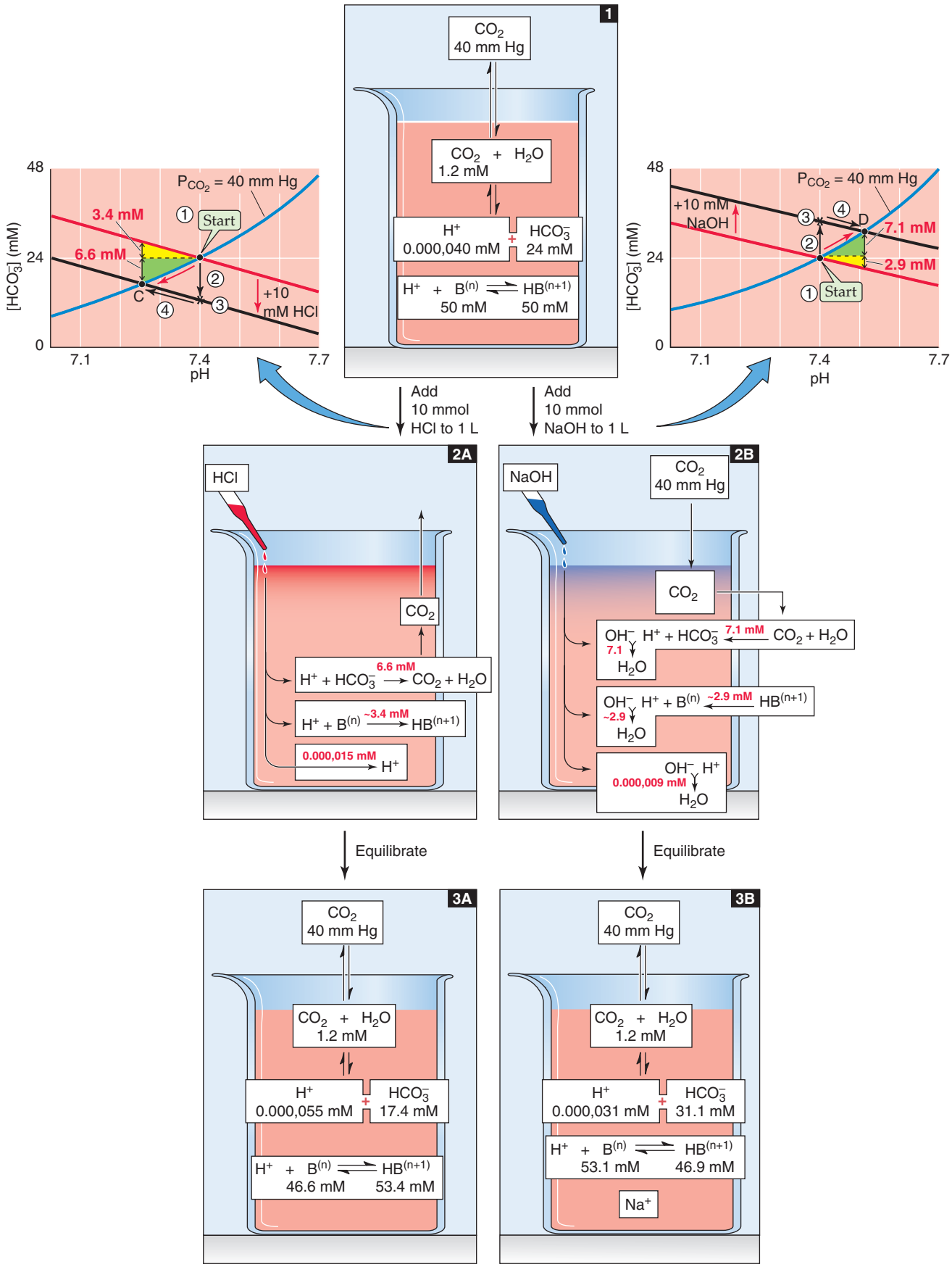

Figure 28-7 Metabolic acidosis and alkalosis in the presence of non-HCO_3^- buffers. The red arrows in the Davenport diagrams represent the transition to metabolic acidosis (point C) and metabolic alkalosis (point D). This example differs from Figure 28-3, in which the solution contained no buffers other than CO_2/HCO_3^-.

TABLE 28-6 Buffering Produced by CO_2/HCO_3^- and Non-HCO_3^- Buffers*

ADDITION	ΔpH	$\Delta[HCO_3^-]$	$\beta_{open}=\frac{\Delta[HCO_3^-]}{\Delta pH}$	$\Delta[B^{(n)}]$	$\beta_{non\text{-}HCO_3^-}=\frac{\Delta[B^{(n)}]}{\Delta pH}$	β_{total}
+10 mmol H^+	~ −0.14	~6.6 mM	47 mM/pH unit	~3.4 mM	25 mM/pH unit	72 mM/pH
+10 mmol OH^-	~ +0.11	~7.1 mM	65 mM/pH unit	~2.9 mM	25 mM/pH unit	89 mM/pH

*The additions are made to 1 L of solution. Initial pH = 7.40, P_{CO_2} = 40 mm Hg, $[HCO_3^-]_o$ = 24 mM. $\beta_{non\text{-}HCO_3^-}$ assumed to be 25 mM/pH unit.

6.6 mmol of the added 10 mmol of H^+ (ΔpH = −0.14). The reason for this difference is that the buffering power of CO_2/HCO_3^- in an open system increases exponentially with pH (see Fig. 28-4, blue curve). In the Davenport diagram, this pH dependence of β_{open} appears as the slope of the CO_2 isopleth, which increases exponentially with pH. *Thus, adding alkali will always cause a smaller pH change than adding an equivalent amount of acid.* In our example of metabolic alkalosis (see right side of Fig. 28-7), the mean β_{open} is (7.1 mM)/(0.11 pH unit) = 65 mM/pH unit in the pH range 7.40 to 7.51 (Table 28-6). On the other hand, in our example of metabolic acidosis (see left side of Fig. 28-7), the mean β_{open} is (6.6 mM)/(0.14 pH unit) = 47 mM/pH unit in the pH range 7.26 to 7.40, substantially less than in the more alkaline range. Because $\beta_{non\text{-}HCO_3^-}$ is 25 mM/pH unit over the entire pH range, β_{total} is greater in the alkaline pH range.

We have already seen that β_{open} is proportional to $[HCO_3^-]$ (see Equation 28-20) and that—at a fixed pH—$[HCO_3^-]$ is proportional to P_{CO_2} (see Equation 28-29). Thus, other things being equal, the contribution of β_{open} to total buffering increases with P_{CO_2}. Patients with a high P_{CO_2} due to respiratory failure will, therefore, have a higher buffering power than normal individuals at the same pH.

Because CO_2/HCO_3^- and non-HCO_3^- buffers compete for added OH^- or H^+, the contribution of CO_2/HCO_3^- to total buffering also depends on $\beta_{non\text{-}HCO_3^-}$. Figure 28-8 illustrates the effects of adding 10 mmol NaOH to our standard 1-L CO_2/HCO_3^- solution at $\beta_{non\text{-}HCO_3^-}$ values of 0, 25 mM/pH unit, and ∞. We saw in Figure 28-3, stage 3B, that adding 10 mmol of NaOH to a 1-L solution containing CO_2/HCO_3^- but no other buffers causes $[HCO_3^-]$ to increase from 24 to 34 mM, and pH to increase from 7.40 to 7.55. To use a Davenport diagram to solve the same problem (see Fig. 28-8*A*), we generate a non-HCO_3^- titration line with slope of zero (because $\beta_{non\text{-}HCO_3^-}$ = 0) through the "Start" point. We also draw a black line with the same slope, but displaced 10 mM higher. Following the blue P_{CO_2} = 40 isopleth from "Start" to the point where the isopleth intersects with the black line at point D_1, we see that—as expected—the final pH is 7.55 and the final $[HCO_3^-]$ is 34 mM. Thus, CO_2/HCO_3^- must buffer virtually all 10 mmol of OH^- added to 1 L. Because the total buffering power is simply β_{open}, the pH increase must be rather large, 0.15.

When $\beta_{non\text{-}HCO_3^-}$ is 25 mM/pH unit, as in the Davenport diagram in the upper right of Figure 28-7 (replotted in Fig. 28-8*B*), CO_2/HCO_3^- can buffer only 7.1 mmol because the non-HCO_3^- buffers neutralize 2.9 mmol. With the increased total buffering power, the pH increase is only 0.11.

Finally, when $\beta_{non\text{-}HCO_3^-}$ is ∞, the black line lies right on top of the vertical non-HCO_3^- titration line (see Fig. 28-8*C*). Thus, neither $[HCO_3^-]$ nor pH changes at all. However,

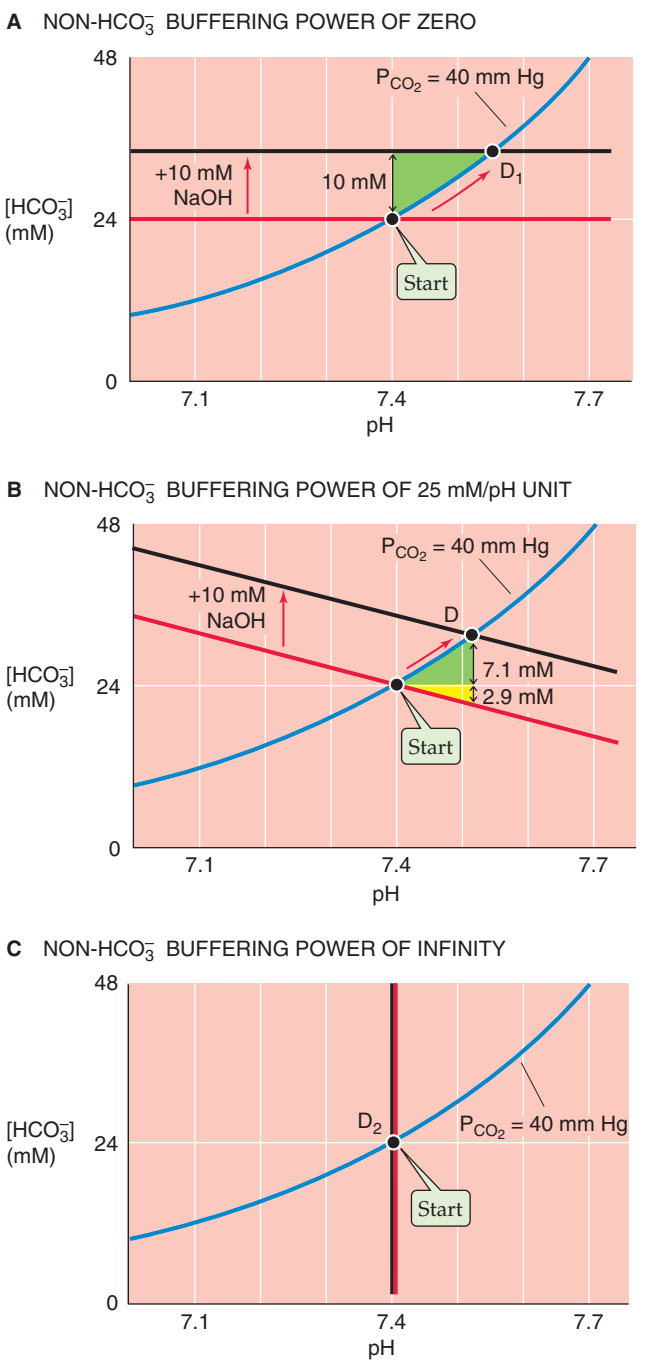

Figure 28-8 Effect of $\beta_{non\text{-}HCO_3^-}$ on the pH increase caused by metabolic alkalosis.

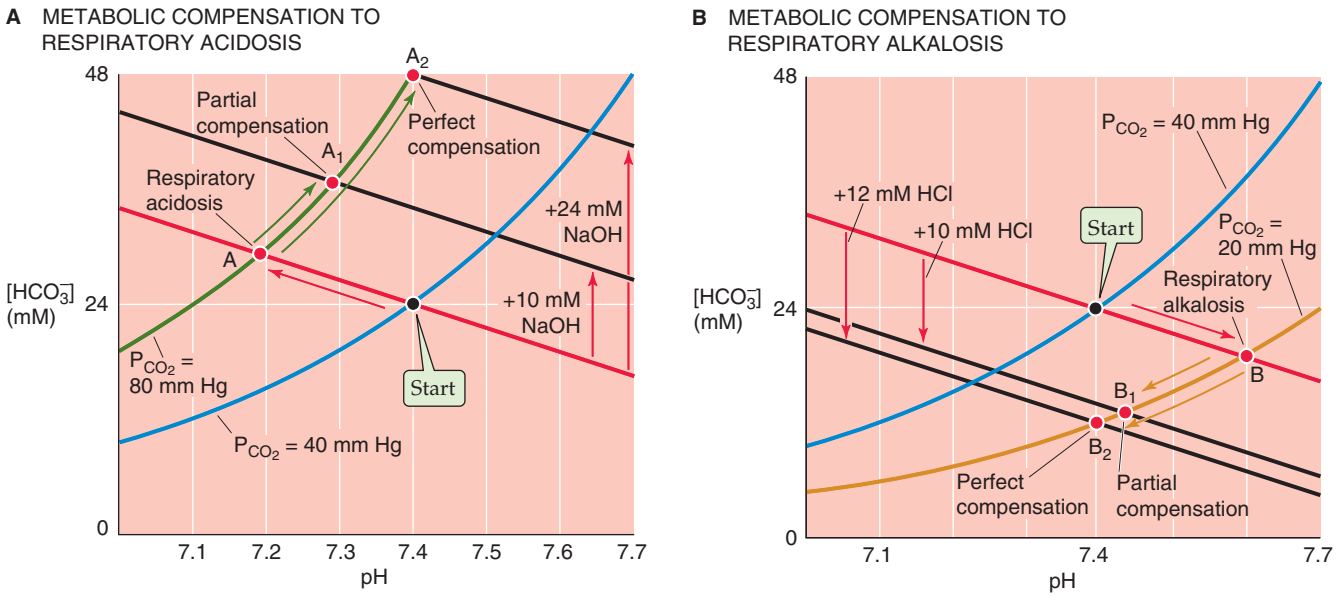

Figure 28-9 Metabolic compensation to primary respiratory acid-base disturbances.

$[HB^{(n+1)}]$ increases by 10 mM because the infinitely powerful non-HCO_3^- buffers do all of the buffering.

This set of three examples—for $\beta_{non\text{-}HCO_3^-}$ values of 0, 25, and ∞—is comparable to the set that we discussed above for *respiratory acidosis* in Figure 28-6*D*.

A metabolic change can compensate for a respiratory disturbance

Thus far, we have considered what happens during *primary* respiratory and metabolic acid-base disturbances. When challenged by such acid or alkaline loads in the blood plasma, the body **compensates** by altering $[HCO_3^-]$ or P_{CO_2}, returning pH toward its initial value and minimizing the magnitude of the overall pH change.

In Figure 28-9*A* we revisit an example, originally introduced in Figure 28-6*C*, in which we produced a primary respiratory acidosis by increasing P_{CO_2} from 40 to 80 mm Hg (red arrow in Fig. 28-9*A* between "Start" and point A at pH 7.19). If the high P_{CO_2} persists, the only way we can restore pH toward its initial value of 7.40 is to add an alkali (e.g., HCO_3^- or OH^-) or remove an acid (e.g., H^+), all of which are equivalent. N28-9 Adding 10 mmol of OH^- to 1 L, for example, superimposes a metabolic *alkalosis* on the primary respiratory *acidosis*—a **metabolic compensation to respiratory acidosis.**

The Davenport diagram predicts the consequences of adding 10 mmol of OH^- to 1 L. We start by generating a black line that is parallel to the red non-HCO_3^- titration line, but displaced upward by 10 mM. Point A_1, the intersection of the black line and the P_{CO_2} isopleth for 80 mm Hg, represents a final pH of 7.29, still lower than the normal 7.40, but much higher than the 7.19 prevailing before compensation.

If we add an additional 14 mmol OH^-, for a total addition of 24 mmol OH^- to 1 L, pH returns to exactly its initial value of 7.40 (point A_2 in Fig. 28-9*A*). In other words, we can perfectly compensate for doubling P_{CO_2} from 40 ("Start") to 80 mm Hg (point A) by adding an amount of OH^- equivalent to the amount of HCO_3^- that was present (i.e., 24 mM) at "Start." *Perfect* compensation of respiratory acidosis is an example of **isohydric hypercapnia** (i.e., *same* pH at a *higher* P_{CO_2}):

$$pH = 6.1 + \log \frac{\overbrace{48\ mM}^{Doubled[HCO_3^-]}}{(0.03\ mM/mm\ Hg) \times \underbrace{80\ mm\ Hg}_{Doubled\ P_{CO_2}}} \quad \textbf{(28-31)}$$

$$= 7.4$$

The kidneys are responsible for the metabolic compensation to a primary respiratory acidosis. They acutely sense high P_{CO_2} and may also chronically sense low blood pH. The response is to increase both the secretion of acid into the urine and the transport of HCO_3^- into the blood (see pp. 832–833), thereby raising plasma pH—a compensatory metabolic alkalosis. The renal compensation to a substantial respiratory acidosis is not perfect, so that pH remains below the normal value of 7.40.

The kidneys can also perform a **metabolic compensation to a respiratory alkalosis.** In Figure 28-9*B* we revisit a second example, originally introduced in Figure 28-6*C*, in which we produced a primary respiratory alkalosis by decreasing P_{CO_2} from 40 to 20 mm Hg (red arrow in Fig. 28-9*B* between "Start" and point B at pH 7.60). We can compensate for most of this respiratory alkalosis by adding 10 mmol of H^+ to each liter of solution or by removing 10 mmol $NaHCO_3$ or NaOH, all of which produce the same effect. We generate a black line that is parallel to the red non-HCO_3^- titration line but is displaced downward by 10 mM. Point B_1 (pH 7.44), at the intersection of the black line and the P_{CO_2} isopleth for 20 mm Hg, represents a partial compensation.

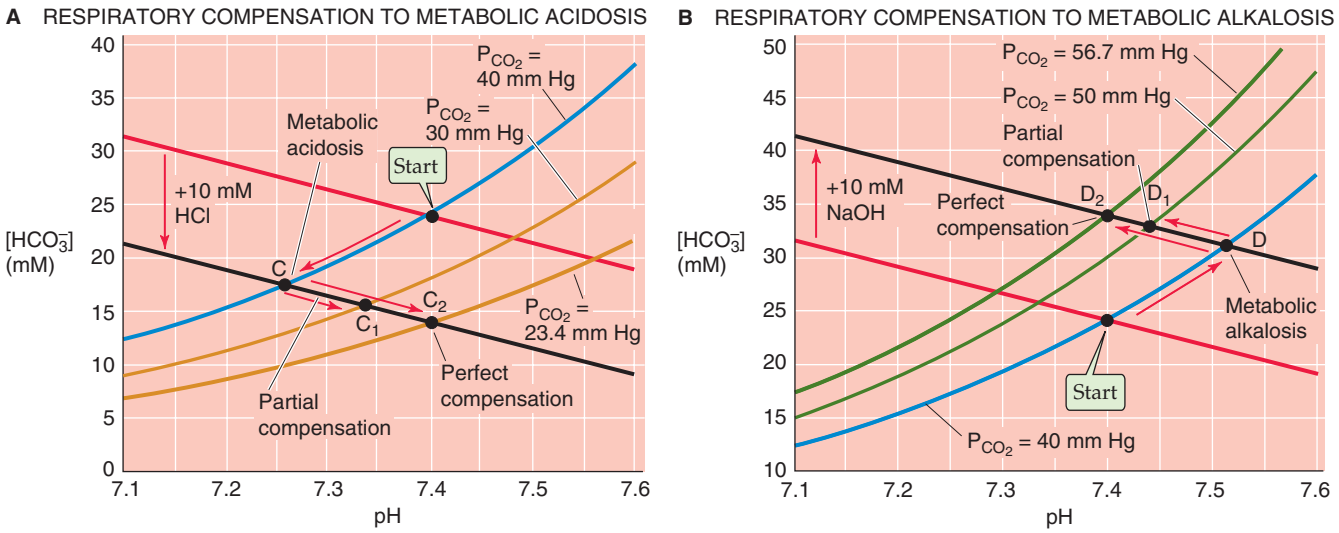

Figure 28-10 Respiratory compensation to primary metabolic acid-base disturbances.

If we add an additional 2 mmol H^+, for a total addition of 12 mmol of H^+ to each liter, pH returns to exactly its initial value of 7.40 (point B_2 in Fig. 28-9*B*). Why is this amount so much less than the 24 mmol of OH^- that we added to each liter to compensate perfectly for a *doubling* of P_{CO_2}? When we halve P_{CO_2}, we need only add an amount of H^+ equivalent to half the amount of HCO_3^- that was present (24/2 = 12 mM) at "Start."

In response to a primary respiratory alkalosis, the kidneys secrete less acid into the urine and transport less HCO_3^- into the blood (see pp. 833–834), thereby lowering plasma pH—a compensatory metabolic acidosis.

A respiratory change can compensate for a metabolic disturbance

Just as metabolic changes can compensate for respiratory disturbances, respiratory changes can compensate for metabolic ones. In Figure 28-10*A* we return to an example originally introduced on the left side of Figure 28-7, in which we produced a primary metabolic acidosis by adding 10 mmol of HCl to 1 L of arterial blood (red arrow in Fig. 28-10*A* between "Start" and point C at pH 7.26). Other than removing the H^+ (or adding OH^- to neutralize the H^+), the only way we can restore pH toward the initial value of 7.40 is to lower P_{CO_2}. That is, we can superimpose a respiratory *alkalosis* on the primary metabolic *acidosis*—a **respiratory compensation to a metabolic acidosis.** For example, we can compensate for most of the metabolic acidosis by reducing P_{CO_2} from 40 to 30 mm Hg. Starting at C, follow the black line from the P_{CO_2} isopleth for 40 mm Hg to the new isopleth for 30 mm Hg at point C_1 (pH 7.34). This maneuver represents a *partial* compensation.

If we reduce P_{CO_2} by an additional 6.6 mm Hg to 23.4 mm Hg, we produce a perfect compensation, which we represent in Figure 28-10*A* by following the black line from C until we reach pH 7.40 at point C_2, which is on the P_{CO_2} isopleth for 23.4 mm Hg. Perfect compensation requires that we reduce P_{CO_2} by a fraction (i.e., [40 − 23.4]/40 ≅ 0.42) that is identical to the ratio of added HCl to the original $[HCO_3^-]$ (i.e., 10/24 ≅ 0.42).

Not surprisingly, the respiratory system is responsible for the respiratory compensation to a primary metabolic acidosis. The low plasma pH or $[HCO_3^-]$ stimulates the peripheral chemoreceptors (see p. 710) and, if sufficiently long-standing, also the central chemoreceptors (see pp. 713–715). The result is an increase in alveolar ventilation, which lowers P_{CO_2} (see pp. 679–680) and thus provides the respiratory compensation.

The body achieves a **respiratory compensation to a primary metabolic alkalosis** in just the opposite manner. In Figure 28-10*B*, we revisit an example originally presented on the right side of Figure 28-7, in which we produce a primary metabolic alkalosis by adding 10 mmol of NaOH to 1 L (red arrow in Fig. 28-10*B* between "Start" and point D at pH 7.51). If we now increase P_{CO_2} from 40 to 50 mm Hg, we partially compensate for the metabolic alkalosis by moving from D to D_1 (pH 7.44). If we raise P_{CO_2} by an additional 6.7 mm Hg to ~56.7 mm Hg, the compensation is perfect, and pH returns to 7.40 (D_2).

In response to a primary metabolic alkalosis, the respiratory system decreases alveolar ventilation and thereby raises P_{CO_2}. The compensatory respiratory acidosis is the least "perfect" of the four types of compensation we have discussed. The reason is that one can decrease alveolar ventilation—and thus oxygenation—only so far before compromising one's very existence.

In a real person, each of the four primary acid-base disturbances—points A, B, C, and D in Figures 28-9 and 28-10—occurs in the extracellular fluid. In each case, the body's first and almost instantaneous response is to use extracellular buffers to neutralize part of the acid or alkaline load. In addition, cells rapidly take up some of the acid or alkaline load and thus participate in the buffering, as discussed below. Furthermore, renal tubule cells may respond to a *metabolic* acidosis of extrarenal origin (e.g., diabetic ketoacidosis) by increasing acid secretion into the urine, or to a metabolic alkalosis (e.g., $NaHCO_3$ therapy) by

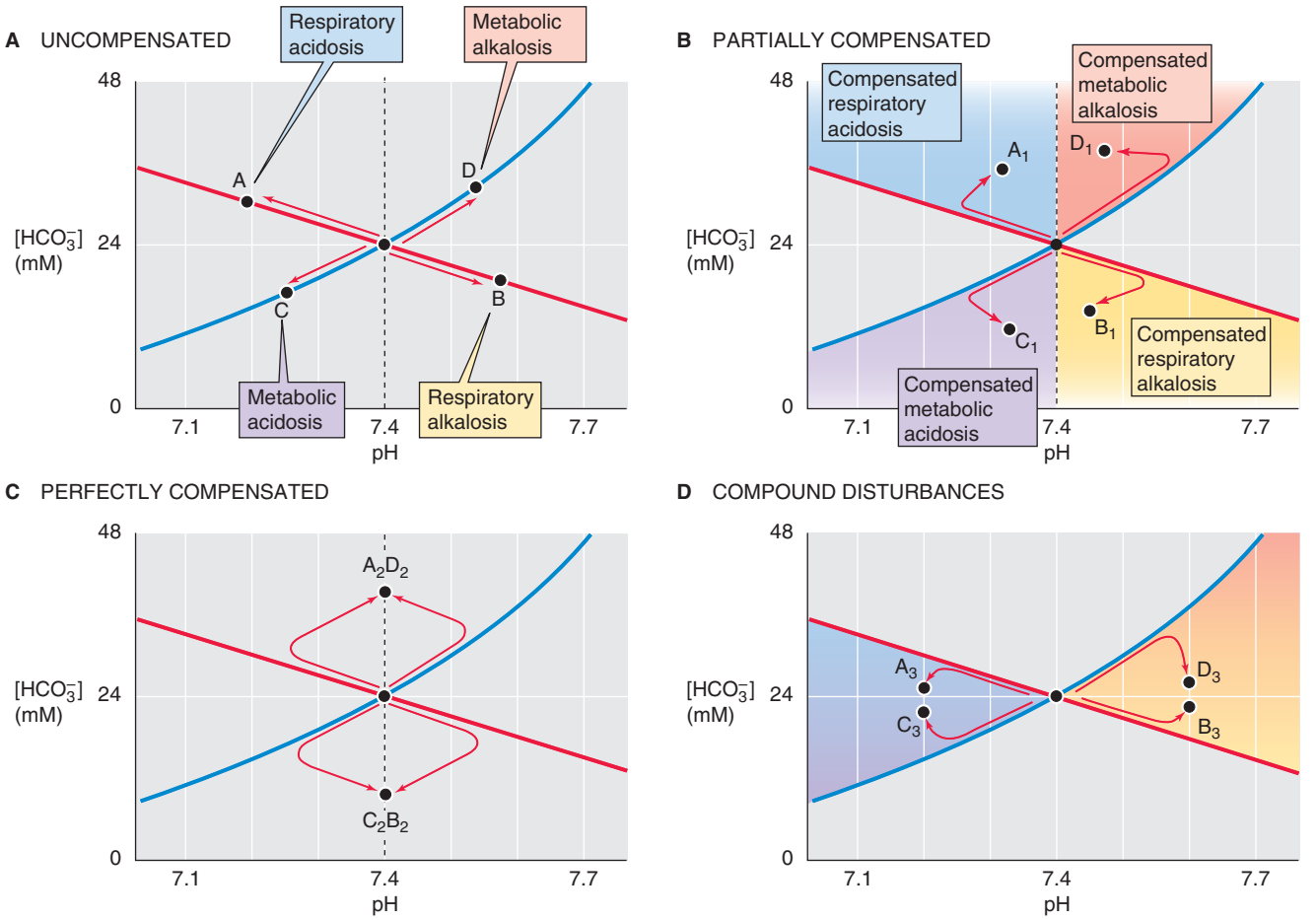

Figure 28-11 Acid-base states represented by position on a Davenport diagram.

decreasing acid secretion—examples of *metabolic* compensation to a *metabolic* disturbance. Points C and D in Figure 28-10 include the effects of the actual acid or alkaline load, extracellular and intracellular buffering, and any renal (i.e., "metabolic") response.

Position on a Davenport diagram defines the nature of an acid-base disturbance

The only tools needed for characterizing acid-base status (i.e., pH, $[HCO_3^-]$, and P_{CO_2}) are a Davenport diagram and electrodes for measuring pH and P_{CO_2}. From these last two parameters, we can compute $[HCO_3^-]$ using the Henderson-Hasselbalch equation. The acid-base status of blood plasma—or of any aqueous solution—must fall into one of five major categories:

1. **Normal.** For arterial blood, pH is 7.40, $[HCO_3^-]$ is 24 mM, and P_{CO_2} is 40 mm Hg. This point was labeled "Start" in the previous figures and is the central point in Figure 28-11*A* through *D*.
2. **One of the four primary (or uncompensated) acid-base disturbances.** The coordinates for pH and $[HCO_3^-]$ fall either (a) on the non-HCO_3^- titration line, but off the 40-mm Hg isopleth for uncompensated respiratory acidosis (point A, Fig. 28-11*A*) or alkalosis (point B); or (b) on the 40-mm Hg isopleth, but off the non-HCO_3^- titration line for an uncompensated metabolic acidosis (point C) or alkalosis (point D).
3. **A partially compensated disturbance.** The coordinates for pH and $[HCO_3^-]$ fall in any of the four colored regions of Figure 28-11*B*. For example, point A_1 in the blue region represents a partially compensated respiratory acidosis. In a subject for whom a respiratory acidosis has existed for longer than a few hours, increased renal H^+ excretion has probably already begun producing a metabolic compensation. Depending on the extent of the original acidosis and the degree of compensation, point A_1 could lie anywhere in the blue region. We can reach similar conclusions for the other three disturbances/compensations.
4. **A perfectly compensated disturbance.** The point falls on the vertical line through pH 7.4. As indicated by point A_2D_2 in Figure 28-11*C*, a perfect compensation following respiratory acidosis is indistinguishable from that following metabolic alkalosis. In either case, the final outcome is isohydric hypercapnia. Similarly, point B_2C_2 represents a perfect compensation following either metabolic acidosis or respiratory alkalosis (isohydric hypocapnia).
5. **A compound respiratory/metabolic disturbance.** The point falls in one of the two colored regions in Figure 28-11*D*. For example, points A_3 and C_3 represent a respiratory acidosis complicated by metabolic acidosis, and

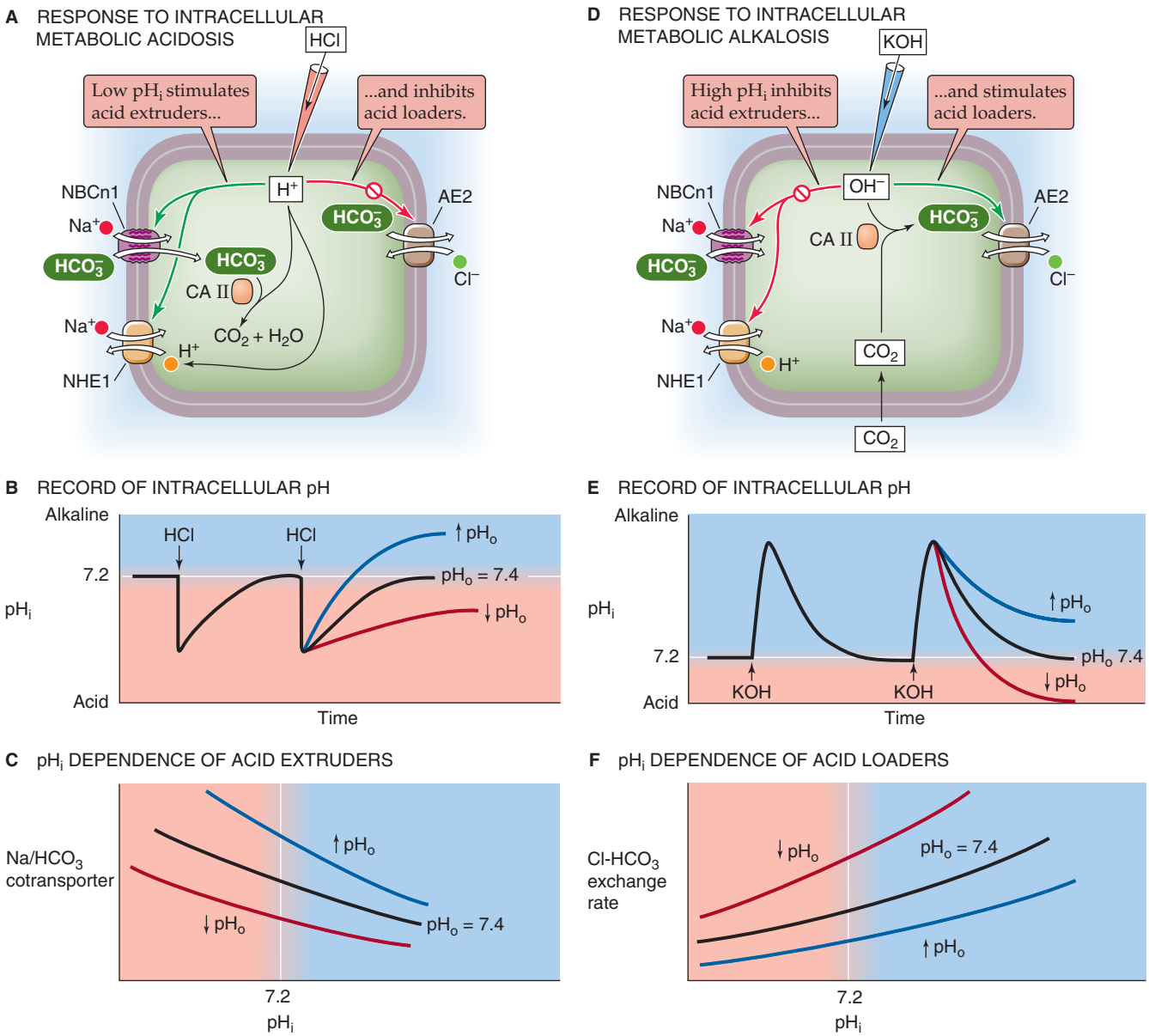

Figure 28-12 Recovery of a cell from intracellular acid and alkali loads. CA II, carbonic anhydrase II.

vice versa. The second disturbance causes the pH to move even further away from "normal," as might occur in an individual with both respiratory and renal failure (see Table 28-3). Of course, it is impossible to determine if one of the two compounding disturbances developed before the other.

pH REGULATION OF INTRACELLULAR FLUID

Clinicians focus on the acid-base status of blood plasma, the fluid compartment whose acid-base status is easiest to assess. However, the number of biochemical reactions and other processes that occur *outside* a cell pales in comparison to the number of those that occur *inside*. It stands to reason that the most important biological fluid for pH regulation is the cytosol. It is possible to monitor intracellular pH (pH_i) continuously in isolated cells and tissues using pH-sensitive dyes or microelectrodes. Moreover, using magnetic resonance techniques, one can monitor pH_i in living humans (e.g., in skeletal muscle). The pH of cells both influences, and is influenced by, extracellular pH.

Ion transporters at the plasma membrane closely regulate the pH inside of cells

Figure 28-12*A* shows a hypothetical cell with three acid-base transporters: an electroneutral Na/HCO_3 cotransporter (NBCn1; see p. 122) a Na-H exchanger (NHE1; pp. 124–125), and a $Cl\text{-}HCO_3$ or anion exchanger (AE2; see p. 124). We will use NBCn1 and NHE1 as prototypic **acid extruders,** transporters that tend to *raise* intracellular pH (pH_i). Both use the energy of the Na^+ gradient to either import HCO_3^- or export H^+ from the cytosol. We will take the $Cl\text{-}HCO_3$

exchanger AE2 as the prototypic **acid loader,** a transporter that tends to *lower* pH_i. AE2, driven by the steep out-to-in Cl^- gradient, moves HCO_3^- out of the cell. The intracellular acid loading produced by Cl-HCO_3 exchange is a **chronic acid load** because it tends to acidify the cell as long as the transporter is active. In our example, the chronic acid extrusion via NBCn1 and NHE1 balances the chronic acid loading via AE2, producing a steady state. Several other acid extruders and acid loaders may contribute to pH_i regulation (see p. 127), and each cell type has a characteristic complement of such transporters.

Imagine that we use a micropipette to inject HCl into the cell in Figure 28-12*A*. This injection of an **acute acid load**—a one-time-only introduction of a fixed quantity of acid—causes an immediate fall in pH_i (see Fig. 28-12*B*, black curve), an example of **intracellular metabolic acidosis.** If we add HCl to a beaker, the pH remains low indefinitely. However, when we acutely acid-load a cell, pH_i spontaneously recovers to the initial value. This pH_i recovery cannot be due to passive H^+ efflux out of the cell, inasmuch as the electrochemical gradient for H^+ (see p. 127) usually favors H^+ influx. Hence, the pH_i recovery reflects the active transport of acid from the cell—a *metabolic compensation to a metabolic acid load.* N28-10

During the recovery of pH_i from the acid load in Figure 28-12*B*, NBCn1 and NHE1not only must extrude the quantity of H^+ previously injected into the cell (the *acute* acid load), they also must counteract whatever acid loading AE2 continues to impose on the cell (the *chronic* acid load).

Acid-extrusion rates tend to be greatest at low pH_i values and fall off as pH_i rises (see Fig. 28-12*C*, black curve). As discussed below, low pH_i also *inhibits* AE2 and thus acid loading. The response to low pH_i therefore involves two feedback loops operating in push-pull fashion, stimulating acid extrusion and inhibiting acid loading.

In addition to pH_i, hormones, growth factors, oncogenes, cell volume, and extracellular pH (pH_o) all can modulate these transporters. The pH_o effect is especially important. In general, a low pH_o slows the rate of pH_i recovery from acute acid loads and reduces the final steady-state pH_i (see Fig. 28-12*B*, red curve), whereas a high pH_o does the opposite (blue curve). The underlying cause of these pH_o effects is a shift of the pH_i dependence of acid extrusion (see Fig. 28-12*C*, red and blue curves) and, as we shall see, changes in acid loading.

Cells also spontaneously recover from acute alkaline loads. If we inject a cell with potassium hydroxide (KOH) (see Fig. 28-12*D*), pH_i rapidly increases but then slowly recovers to its initial value (see Fig. 28-12*E*, black curve), which reflects stimulation of acid loading and inhibition of acid extrusion. The injection of OH^- represents a metabolic alkalosis, whereas increased Cl-HCO_3 exchange represents a metabolic compensation. N28-10 The Cl-HCO_3 exchanger is most active at high pH_i values (see Fig. 28-12*F*). As discussed previously, increases in pH_i generally inhibit acid extruders. Thus, the response to alkaline loads—like the response to acid loads—includes dual feedback loops operating in push-pull fashion, stimulating acid loading and inhibiting acid extrusion. During the pH_i recovery from an acute alkaline load, Cl-HCO_3 exchange not only must neutralize the alkali previously injected into the cell (the acute alkali load), but also must counteract the alkalinizing effect of acid extruders such as the Na/HCO_3 cotransporter.

Like acid extruders, Cl-HCO_3 exchangers are under the control of hormones and growth factors with a pH_o sensitivity that is opposite to that of the acid extruders (i.e., low pH_o enhances Cl-HCO_3 exchange). In general, an extracellular metabolic acidosis, with its simultaneous fall in *both* pH_o and [HCO_3^-] (see Table 28-3), stimulates acid loading via Cl-HCO_3 exchange (see Fig. 28-12*F*, red curve). During the recovery from acute alkali loads, metabolic acidosis therefore causes pH_i to fall more rapidly and to reach a lower steady-state value (see Fig. 28-12*E*, red curve).

Indirect interactions between K^+ and H^+ make it appear as if cells have a K-H exchanger

Clinicians have long known that extracellular acidosis leads to a release of K^+ from cells, and thus hyperkalemia (see p. 795). Conversely, hyperkalemia leads to the exit of H^+ from cells, resulting in extracellular acidosis. These observations, which one can duplicate in single, isolated cells, led to the suggestion that cells generally have K-H exchangers. It is true that specialized cells in the stomach (see pp. 865–866) and kidney (see pp. 827–828) do have an ATP-driven pump that extrudes H^+ in exchange for K^+. Moreover, the K/HCO_3 cotransporter described in certain cells could mimic a K-H exchanger. Nevertheless, the effects that long ago led to the K-H–exchange hypothesis probably reflect *indirect* interactions of H^+ and K^+.

One example of apparent K-H exchange is that hyperkalemia causes an intracellular alkalosis. Not only is this effect *not* due to a 1:1 exchange of K^+ for H^+, it is not even due to the increase in $[K^+]_o$ per se. Instead, the high $[K^+]_o$ depolarizes the cell, and this positive shift in membrane voltage can promote events such as the net uptake of HCO_3^- via the electrogenic Na/HCO_3 cotransporter (see p. 122) and thus a rise in pH_i—a **depolarization-induced alkalinization.** Depolarization also can indirectly stimulate other transporters that alkalinize the cell. We discuss the converse example of acidemia causing hyperkalemia on page 795: Extracellular acidosis lowers pH_i and inhibits transporters responsible for K^+ uptake, which leads to net K^+ release from cells. Although we have no evidence that a K-H exchanger exists in humans, imagining that it exists is sometimes a helpful tool for quickly predicting interactions of H^+ and K^+ in a clinical setting.

Changes in intracellular pH are often a sign of changes in extracellular pH, and vice versa

By definition, acid extrusion (e.g., Na/HCO_3 cotransport) equals acid loading (e.g., Cl-HCO_3 exchange) in the steady state. Disturbing this balance shifts pH_i. For example, extracellular *metabolic* acidosis inhibits acid extrusion and stimulates acid loading, thus lowering steady-state pH_i. This intracellular acidosis is not instantaneous, but develops over a minute or two. Conversely, extracellular metabolic alkalosis leads to a slow increase in steady-state pH_i. Generally, a change in pH_o shifts pH_i in the same direction, but ΔpH_i is usually only 20% to 60% of ΔpH_o. In other words, an extracellular metabolic acidosis causes a net transfer of acid from the extracellular to the intracellular space, and an

N28-10 Acid Extruders and Acid Loaders in a Cell

Contributed by Emile Boulpaep and Walter Boron

Of the acid extruders that can produce pH_i recovery, the most widely distributed is the NHE1 isoform of the Na-H exchanger. However, mechanisms that mediate HCO_3^- uptake often coexist with the Na-H exchanger in the same cell and are sometimes far more powerful than the Na-H exchanger. These HCO_3^- transporters include the Na^+-driven Cl-HCO_3 exchanger (or NDCBE, illustrated in Fig. 5-14, no. 17) and the Na/HCO_3 cotransporters with Na^+:HCO_3^- stoichiometries of 1 : 2 (NBCe1 and NBCe2, the electrogenic Na/HCO_3 cotransporters) and 1 : 1 (NBCn1, the electroneutral Na/HCO_3 cotransporter). Note that the electrogenic Na/HCO_3 cotransporter that operates with an Na^+:HCO_3^- stoichiometry of 1 : 3 (see Fig. 5-14, no. 19) mediates net HCO_3^- efflux—which reflects the ionic and electrical gradients that govern its thermodynamic properties—and functions as an acid loader. However, the Na/HCO_3 cotransporters with Na^+:HCO_3^- stoichiometries of 1 : 2 and 1 : 1 both mediate the net uptake of HCO_3^- and function as acid extruders.

Other transporters that extrude acid from cells include the V-type H pump and the H-K exchange pump.

Other transport processes that acid-load cells include the passive influx of H^+ as well as the efflux of HCO_3^- either through channels (e.g., gamma-aminobutyric acid or glycine-activated Cl^- channels) or through the K/HCO_3 cotransporter.

For a more detailed discussion of these transporters, see page 127.

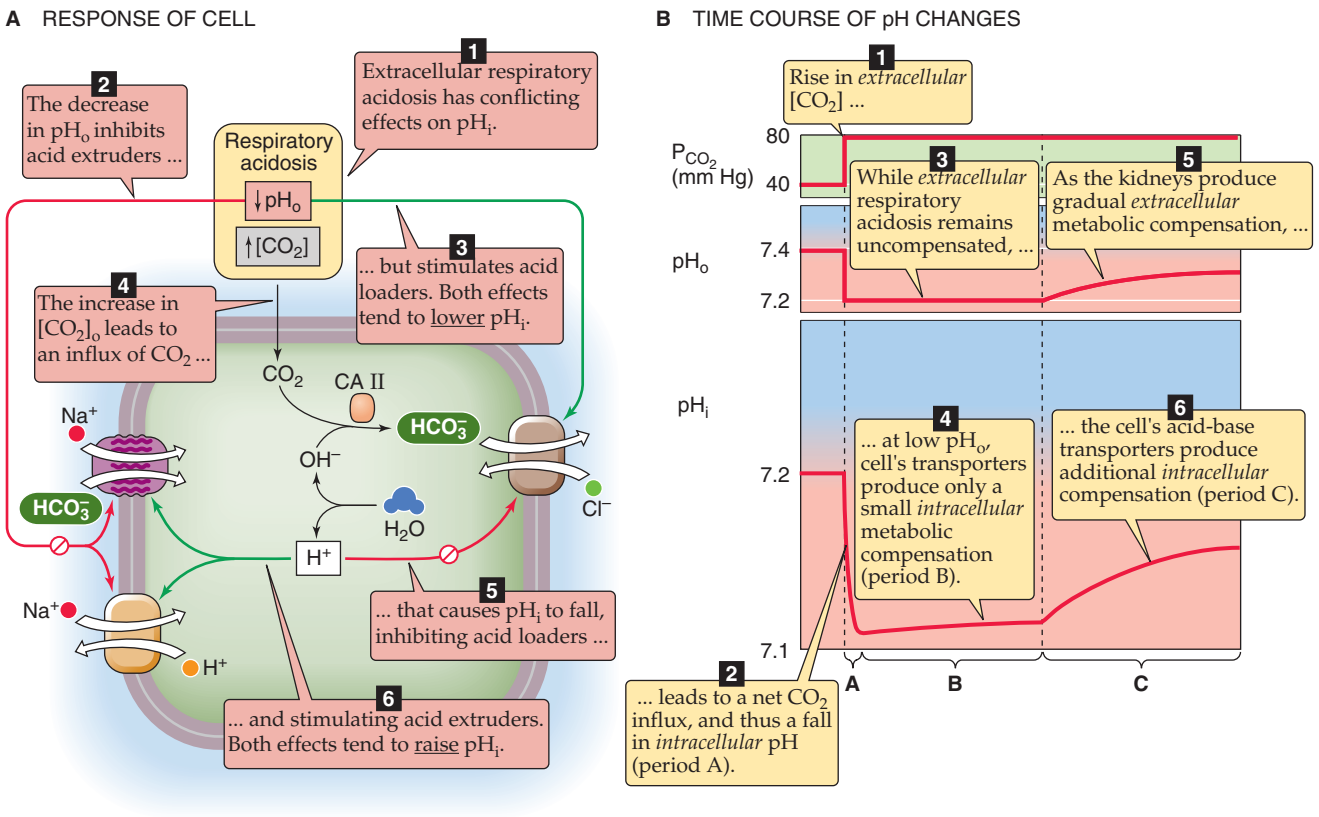

Figure 28-13 Response of cell to extracellular respiratory acidosis.

extracellular metabolic alkalosis has the opposite effect. Thus, cells participate in buffering extracellular acid and alkali loads.

Extracellular *respiratory* acidosis generally affects pH_i in three phases. First, the increase in extracellular $[CO_2]_{dis}$ creates an inwardly directed gradient for CO_2. This dissolved gas rapidly enters the cell (Fig. 28-13*A*) and produces HCO_3^- and H^+. This **intracellular respiratory acidosis** manifests itself as a rapid fall in pH_i (see Fig. 28-13*B*, phase A in lower panel). Carbonic anhydrase N18-3 greatly accelerates the formation of HCO_3^- and H^+ from CO_2, so that pH_i can complete its decline in just a few seconds.

The cell recovers from this acid load, but only feebly (see Fig. 28-13*B*, phase B in lower panel) because the decrease in pH_o inhibits acid extrusion and stimulates acid loading. Over a period of minutes, pH_i may recover only partially if at all.

Finally, the extracellular respiratory acidosis stimulates the kidneys to upregulate acid-base transporters and thus stimulate urinary acid secretion (see p. 832). The net effect, over a period of hours or days, is an extracellular metabolic compensation that causes pH_o to increase gradually (see Fig. 28-13*B*, phase C in upper panel). As pH_o rises, it gradually relieves the inhibition of NBCn1 and NHE1 and other acid extruders and cancels the stimulation of Cl-HCO_3 exchange and other acid loaders. Thus, *intra*cellular pH recovers in parallel with *extra*cellular pH, albeit by only 20% to 60% as much as pH_o (see Fig. 28-13*B*, phase C in lower panel). The pH_i recovery represents an **intracellular metabolic compensation** to the intracellular respiratory acidosis.

Not all cell types have the same resting pH_i. Moreover, different cell types often have very different complements of acid-base transporters and very different ways of regulating these transporters. Nevertheless, the example in Figure 28-13 illustrates that the fate of pH_i is closely intertwined with that of interstitial fluid, and thus blood plasma. During respiratory acid-base disturbances, the lungs generate the insult, and virtually every other cell in the body must defend itself against it. In the case of metabolic acid-base disturbances, however, some cells may generate the insult, whereas the others attempt to defend themselves against it. From a teleological perspective, one can imagine that the primary reason that the body regulates the pH of the blood plasma and extracellular fluids is to allow the cells to properly regulate their pH_i. The primary reason why the clinical assessment of blood acid-base parameters can be useful is that these parameters tend to parallel cellular acid-base status.

REFERENCES

The reference list is available at www.StudentConsult.com.

REFERENCES

Books and Reviews

Bevensee MO, Alper S, Aronson PS, Boron WF: Control of intracellular pH. In Seldin DW, Giebisch G (eds): The Kidney: Physiology and Pathophysiology, 3rd ed. Philadelphia, Lippincott Williams & Wilkins, 2000, pp 391–442.

Busa WB, Nuccitelli R: Metabolic regulation via intracellular pH. Am J Physiol 246:R409–R438, 1984.

Davenport HW: The ABC of Acid Base Chemistry, 6th ed. Chicago, University of Chicago Press, 1974.

Mount DB, Romero MF: The SLC26 gene family of multifunctional anion exchangers. Pflugers Arch 447:710–721, 2004.

Orlowski J, Grinstein S: Diversity of the mammalian sodium/proton exchanger SLC9 gene family. Pflugers Arch 447:549–565, 2004.

Romero MF, Fulton CM, Boron WF: The SLC4 family of HCO_3^- transporters. Pflugers Arch 447:495–509, 2004.

Roos A, Boron WF: Intracellular pH. Physiol Rev 61:296–434, 1981.

Sly WS, Hu PY: Human carbonic anhydrases and carbonic anhydrase deficiencies. Annu Rev Biochem 64:375–401, 1995.

Vaughan-Jones RD, Boron WF: Integration of acid-base and electrolyte disorders. New Engl J Med 372:389, 2015.

Wakabayashi S, Shigekawa M, Pouysségur J: Molecular physiology of vertebrate Na^+/H^+ exchangers. Physiol Rev 77:51–74, 1997.

Journal Articles

Boron WF, De Weer P: Intracellular pH transients in squid giant axons caused by CO_2, NH_3, and metabolic inhibitors. J Gen Physiol 67:91–112, 1976.

Sørensen SPL: Über die Messung und die Bedeutung der Wasserstoffi-onenkonzentration bei enzymatischen Prozessen. Biochem Z 21:131–200, 201–304, 1909.

Thomas RC: The effect of carbon dioxide on the intracellular pH and buffering power of snail neurones. J Physiol 255:715–735, 1976.

Zhao J, Hogan EM, Bevensee MO, Boron WF: Out-of-equilibrium CO_2/HCO_3^- solutions and their use in characterizing a novel K/HCO_3 cotransporter. Nature 374:636–639, 1995.